Unchanged surface morphology in debris-covered glaciers and rock glaciers in Tröllaskagi peninsula (northern Iceland)

Luis M. Tanarro[1]*, David Palacios[1], Nuria Andrés[1], José M. Fernández-Fernández[1], José J. Zamorano[2], Þorsteinn Sæmundsson[3], Skafti Brynjólfsson[4]

[1]Research Group of High Mountain Physical Geography. Departament of Geography, Universidad Complutense de Madrid, Madrid, 28040 Madrid, Spain.

[2]Institute of Geography, Universidad Nacional Autónoma de México. México DF. Mexico

[3]Faculty of Life and Environmental Science, University of Iceland, Reykjavík, Iceland

[4]Icelandic Institute of Natural History, Akureyri, Iceland

* Corresponding author

Luis M. Tanarro, pace@ghis.ucm.es

Department of Geography,

Complutense University of Madrid

Profesor Aranguren st, Ciudad Universitaria s/n, 28040, Madrid, Spain

Tel: + 34 91 394 77 93

ABSTRACT

This paper analyses changes in the surface morphology of rock and debris-covered glaciers in the Hóladalsjökull and Fremri-Grjótárdalur cirques near Hólar village in the Tröllaskagi peninsula (northern Iceland) (65°43′55″N; 19°06′49″W, 160 m), to understand the dynamics and climatic significance of these landforms. The study includes an analysis of historical aerial photographs from 1946 to 2000. The aim was to evaluate surface changes in these landforms and obtain the horizontal displacement and elevation changes of large boulders and linear features (ridges and furrows) at each date. In addition, the surface elevation differences between 1980 and 1994 were obtained from digital elevation models. The horizontal displacement results obtain a mean velocity of 0.33 m yr^{-1} and an average elevation difference of -0.72 m for the boulders, with the linear features advancing 14.84 m during the period 1946-2000. Except for this slow mobility, no changes occurred in the surface morphology of these landforms

during the 54 years. The low displacement rates of boulders and linear features, together with the surface lowering processes observed in these landforms, indicate that widespread melting is the most important activity in the debris-covered and rock glaciers in Tröllaskagi. This is confirmed by the recent formation of collapse depressions.

Key words: debris-covered glacier, rock glacier, themokarst depressions, digital photogrammetry, boulder displacement, elevation change, Tröllaskagi peninsula, Iceland

1. Introduction

The Tröllaskagi peninsula hosts 167 alpine glaciers (Icelandic Meteorological Office, 2018), mostly north-facing (Sigurðsson and Williams, 2008). A few of these glaciers are debris-free, but most are debris-covered or end in a rock glacier (Björnsson, 1991; Wangensteen et al., 2006; Kellerer-Pirklbauer et al., 2007; Björnsson and Pálsson, 2008). Although the recent glacier evolution of Iceland is well known (see synthesis in Ingólfsson and Norddahl, 1994; Geirsdóttir et al., 2009; Geirsdóttir, 2011; Pétursson et al., 2015), the origin of the Tröllaskagi debris-covered and rock glaciers is still under discussion. Initial research into these debris-covered and rock glaciers was carried out especially during the 1970s-1990s. For some researchers, the rock glaciers formed recently, during the Little Ice Age (LIA) expansion, and are approximately 200 years old, according to lichenometric criteria and present mobility rates (Martin et al., 1994; Hamilton and Whalley, 1995a, 1995b). This young age has also been deduced from the depression of the glacial Equilibrium Line Altitude (ELA) in Tröllaskagi (Ipsen et al., 2018). However, other authors estimate the oldest age for these Tröllaskagi debris-covered and rock glaciers to be around 6 ka or even older according to streamlines based on the displacement field and surface velocities from 1985–1994 data (Wangensteen et al., 2006; Kellerer-Pirklbauer et al., 2007).

Debris-free glaciers, rock glaciers and debris-covered glaciers in Tröllaskagi coexist in cirques in close proximity. The limits of these three glacier types and their genetic relationships are still not clear (Berthling, 2011; Janke et al., 2015). A glacier becomes a debris-covered glacier when supraglacial debris more than 0.5 m thick covers more than 50% of the ablation area (Azócar and Brenning, 2010; Brenning, 2005; Hambrey et al.,

2008; Kirkbride, 2011, 2000). The differences between debris-covered glaciers and rock glaciers are even less clear; they are considered to be rock glaciers where the surface debris layer is thicker than debris-covered glaciers and the ice content is estimated to be less than 30% of the total mass (Haeberli et al., 2006; Berthling, 2011). The difference in surface morphology is not clearly defined, but ridges on debris-covered glaciers tend to be more longitudinal, while lateral and central moraines are still evident and some viscous flow morphology is observed (Clark et al., 1994). In addition, rock glacier morphology is defined by the existence of pronounced transverse ridges and furrows, perpendicular to the flow direction (Capps, 1910; Wahrhaftig and Cox, 1959; Vitek and Giardino, 1987; Martin and Whalley, 1987; Whalley and Martin, 1992; Barsch, 1992, 1996; Hamilton and Whalley, 1995a, 1995b; Haeberli et al., 2006; Berthling, 2011; Janke et al., 2013; Monnier and Kinnard, 2017).

Applying these criteria to Tröllaskagi, the current dynamics and geomorphological context of rock glaciers and debris-covered glaciers are quite similar. There are no moraine ridges in cirques with rock glaciers and debris-covered glaciers, but many occur in valleys where debris-free glaciers exist (Hamilton and Whalley, 1995a, 1995b; Martin et al., 1991; Andrés et al., 2016). Aerial photos from different dates do not show geomorphic evidence of change to their surface morphology (Hamilton and Whalley, 1995a, 1995b; Andrés et al., 2016) and advances and changes of their fronts are not apparent (Whalley et al., 1995a, 1995b; Andrés et al., 2016). Nevertheless, these observations of the absence of surface changes in debris-covered and rock glaciers contradict the analysis by some authors using photogrammetric techniques, obtaining surface boulder displacement up to 0.84 m yr^{-1} (Kellerer-Pirklbauer et al., 2007; Wangensteen et al., 2006) or up to 3 m yr^{-1} using satellite radar interferometry (Lilleøren et al., 2013). Other authors consider that Tröllaskagi debris-free glaciers are very dynamic and that their fronts are highly sensitive to climate fluctuations (Caseldine, 1985; Eyþórsson, 1935, 1931; Fernández-Fernández et al., 2017). The retreat of nearby debris-free glaciers from the LIA moraines to the present margins averages around 1300 m (Fernández-Fernández et al., 2017). This retreat was interrupted during at least five cold periods with glacier snout advances which formed many frontal moraines (Caseldine, 1983, 1985; Eyþórsson, 1935; Fernández-Fernández et al., 2017). However, various surge-type glaciers have been described in Tröllaskagi,

forming several frontal moraines in the area, and therefore their origin is not directly related to climate evolution (Björnsson et al., 2003; Brynjólfsson et al., 2012).

One of the key factors when studying the origin and climatic significance of rock glaciers and debris-covered glaciers is the analysis of their dynamics and morphological changes over time (Benn et al., 2012; Bosson and Lambiel, 2016; Brenning, 2005; Capt et al., 2016; Deline, 2005; Emmer et al., 2015; Humlum, 1998; Kääb, 2008; Kellerer-Pirklbauer et al., 2008; Kellerer-Pirklbauer and Kaufmann, 2012). The aim of this present research is to study the evolution and morphodynamics of a rock glacier and a debris-covered glacier in the Tröllaskagi peninsula to gain a better understanding of the differences, origin and climatic significance of these formations, using an innovative approach. To achieve this aim, a range of consistent photogrammetric techniques and geographic information system (GIS) analyses are applied in a multi-temporal approach involving processing and comparison of historical aerial photographs.

2. Regional setting

The Tröllaskagi peninsula in north central Iceland lies between meridians 19º30'W and 18º10'W, jutting out into the North Atlantic to latitude 66º12'N and linked to the central Icelandic Highlands to the south, between the Skagafjörður fjord to the west and the Eyjafjörður fjord to the east (Fig. 1A). The peninsula is a plateau, topped by flat summits and ridges, intensely dissected by the drainage network, which forms flat-bottomed valleys, often with steep walls. It is composed of Tertiary basalt bedrock, with semi-horizontal lava flows often separated by 30-50 cm thick lithified, mainly argillaceous, sedimentary horizons known as red interbed layers (Sæmundsson et al., 1980). The slopes are often unstable, as many are affected by rock slope failures and deep-seated gravitational slope deformation, often of significant magnitude, where the red interbed layers act as decollement levels (Cossart et al., 2014; Feuillet et al., 2014; Jönsson, 1976; Whalley et al., 1983). These macro-mass movements are considered to have developed as a result of the final deglaciation during the early Holocene (Coquin et al., 2015; Cossart et al., 2014; Mercier et al., 2013) and some of them are still active (Sæmundsson et al., 2007; Wangensteen et al., 2006). Large scale failure events may originate in cirque headwalls in Tröllaskagi and the resulting landforms resemble rockglaciers (Sigurdsson, 1990; Whalley et al., 1983; Whalley and Martin, 1992).

The climate of the Tröllaskagi peninsula is characterized by a mean annual air temperature (MAAT) of 2 to 4 ºC (1961–1990 data series) on the Tröllaskagi coasts and of -2 to -4 ºC on the summits (Etzelmüller et al., 2007). The precipitation is relatively low, because the central highland and the ice-caps block the wet southerly winds.The precipitation is mainly contributed by northerly winds and oscillates between 400 mm in some lowland areas and 2000 mm on the summits (1971–2000 data series) (Crochet et al., 2007). The continuous permafrost limit in the Tröllaskagi mountains has been modeled and located between 850-950 m a.s.l. (Etzelmüller et al., 2007; Wangensteen et al., 2006). The termini of most of the debris-covered and rock glaciers are at 900-950 m a.s.l., where the MAAT is -1.8 to -2.6 ºC (extrapolated with a gradient of -0.65 ºC 100 m^{-1} from Hólar í Hjaltadal meteorological station at 160 m a.s.l.,1961–1990) (Kellerer-Pirklbauer et al., 2007) with precipitation around 1500 mm (Crochet et al., 2007). The current ELA of the main debris-free glaciers is 1010-1060 m a.s.l., with MAAT around -2.3 ºC at the ELA (Fernández-Fernández et al., 2017). These glaciers reached their LIA maximum approx. 1865-1900 (Caseldine, 1985), with an ELA of 950-1010 m a.s.l. and MAAT 1.7-1.9 ºC lower than at present (Caseldine and Stötter, 1993; Fernández-Fernández et al., 2017).

3. Selection of the case study landforms and previous studies.

The rock glacier that has attracted most attention of researchers in Tröllaskagi is Nautárdalur (65°29'21"N 18°22'14"W, altitude 1300-940 m a.s.l.), studied and monitored in 1977-1994 (Hamilton and Whalley, 1995a, 1995b; Martin and Whalley, 1987; Martin et al., 1994, 1991). It is located in a cirque on the north slope of Skjóldalur, a tributary valley of the Eyjafjörðurfjord from the west, 20 km south of Akureyri (Fig. 1A). Significant research has been carried out in two other cirques (Farbrot et al., 2007; Kellerer-Pirklbauer et al., 2007; Lilleøren et al., 2013; Wangensteen et al., 2006), both north-facing in the Hóladalur valley, a tributary of the Skagafjörðurfjord from the east, 7 km west of Hólar village (Fig. 1B and 1C). The western cirque, Fremri-Grjótárdalur, (65°43' N 19° W, 1245 m a.s.l.) hosts a series of active rock glaciers, and the eastern cirque hosts the debris-covered glacier Hóladalsjökull (65°42' N; 18°57' W, 1330 m a.s.l.).

Important differences in the results and interpretations were detailed by authors who worked in Nautárdalur and those who worked on the Hólar rock glaciers, in relation to the origin, dynamics and age of these landforms:

I Origin. -Nautárdalur was considered a rock glacier derived from a small corrie glacier after frequent rock falls, which supplied mantled debris on the glacial surface. A similar origin was attributed to the other Tröllaskagi rock glaciers (Martin and Whalley, 1987; Martin et al., 1991; Whalley and Martin, 1994; Hamilton and Whalley, 1995a, 1995b;). Extrapolation from the Akureyri long-term meteorological temperature data to Nautárdalur cirque, with MAAT <-2ºC, showed that permafrost is only possible on snow-blown summit plateau areas (1250-1300 m a.s.l.), even during the LIA (Whalley and Martin, 1994). Authors working in the Hólar area considered that some rock glaciers derived from debris-free glaciers, but others were formed from slope talus with segregate ground ice. In any case, permafrost is present in the cirques, following the conclusions of Etzelmüller et al. (2007), who established the permafrost limit at 800-900 m on Tröllaskagi during the LIA, 200–300 m lower than today. Farbrot et al. (2007) support this idea with direct data logger measurements. Lilleøren et al. (2013) calculated the MAAT around -4ºC at the roots of Tröllaskagi rock glaciers.

II Dynamics. -Nautárdalur glacier was considered almost static. Boulder movement measured by theodolite for seventeen years ranges from <0.05 m yr^{-1} to 0.31 m yr^{-1} and the snout advanced <1 m during this period (Whalley et al., 1995a, 1995b). Different conclusions were reached in the Hólar area by Wangensteen et al. (2006), who applied digital photogrammetry and cross-correlation matching of multi-temporal orthophotos from 1985 and 1994, and obtained block movement ranging from 0.07 m yr^{-1} to 0.84 m yr^{-1} on the Hóladalsjökull debris coevered glacier and Fremri-Grjótárdalur rock glaciers, respectively. Kellerer-Pirklbauer et al. (2007) used similar techniques in Fremri-Grjótárdalur rock glaciers and obtained similar results ranging from 0.06 m yr^{-1} to 0.74 m yr^{-1}. Lilleøren et al. (2013) used satellite radar interferometry (ALOS polarimetric PALSAR images 16 August-1 October 2007) and normally obtained block movement of 0.2–0.5 m yr^{-1} when applied in some rock glaciers in Tröllaskagi, with maximum velocities exceeding 3 m yr^{-1}.

III Age.- From headwall recession rate and lichenometric dating, some authors deduced that the maximum age of the Nautárdalur rock glacier is approximately 200 yr BP and

was related to the LIA expansion (Martin et al., 1994; Hamilton and Whalley, 1995a, 1995b;). Authors working on the Hóladalsjökull debris covered glacier and the Fremri-Grjótárdalur rock glaciers proposed headwall recession rates from 0.4 to 1.2 mm a^{-1} in these cirques (Farbrot et al., 2007). Other authors made streamline interpolations from surface velocities (Wangensteen et al., 2006; Kellerer-Pirklbauer et al., 2007), and relative surface dating using a Schmidt-hammer (Kellerer-Pirklbauer et al., 2008). Wangensteen et al. (2006) estimated 4.5-5 ka as the oldest age for these landforms, with reactivation of the higher lobes at 1000-1500 yr. For the Fremri-Grjótárdalur fossil rock glacier, Kellerer-Pirklbauer et al. (2007) proposed an age contemporary with the GH-8.2 event (8.6-8.0 ka cal. yr BP according to Greenland stratigraphy). However, the origin of the active rock glacier was related to one of the first neoglacial Tröllaskagi advances of ca. 5.2 to 5.9 ka cal. yr BP. The reactivation of the higher lobes took place during the second neoglacial advance by 3.0-3.2 ka (Kellerer-Pirklbauer et al., 2007).

IV Relationship between debris-covered and rock glaciers and past cold periods. Hamilton and Whalley (1995a, 1995b) noted the absence of moraines in front of the Nautárdalur rock glacier, and in other Tröllaskagi cirques including rock glaciers. They also observed a large spoon-shaped depression in the upper region of the Nautárdalur rock glacier, which occurs in many other Tröllaskagi rockglaciers. They consider that the origin of these head basins is related to post-LIA glacial recession. Other authors have inferred that these glaciers formed during the first Holocene cold phases, after the Holocene Thermal Maximum (HTM) (Wangensteen et al., 2006; Kellerer-Pirklbauer et al., 2007). Recent cosmogenic dating of boulders from some small moraines, fossil rock glaciers and erratic boulders close to the present debris-covered and rock glaciers in Tröllaskagi suggests that during the Oldest Dryas, Younger Dryas and Early Preboreal, small glaciers formed in Tröllaskagiin the interior of the cirques, which were not more than 1-3 times larger than present-day glaciers, and were not connected through the tributary valleys to the main fjords at those times (Andrés et al., 2016).

For this case study, the rock glaciers located in Fremri-Grjótárdalur and the Hóladalsjökull debris-covered glacier were selected. These are located just north of Hólar village, hosted in adjacent cirques at the head of the Hóladalur valley. These cirques are bounded by prominent cliffs, with summits reaching 1200-1330 m a.s.l. At the foot of these 100-170 m high north-facing cirque-walls, there are small corrie glaciers with spoon-shaped hollows where the rock glacier and debris-covered glaciers

developed (Fig. 1B and C and Fig. 2A). The debris-cover thickness of Hóladalsjökull can be observed in several collapse depressions (Fig. 3A). Fremri-Grjótárdalur rock glaciers have layers of debris that rest on segregate ice (Farbrot et al., 2007). These rock glaciers are formed by blocks with a clay matrix and average diameter of 40 cm, although some may have a diameter as large as 3 m (Kellerer-Pirklbauer et al., 2007).

4. Methods and materials

In recent years, with digital photogrammetry the displacement and recent changes in the superficial morphology of rock glaciers and debris-covered glaciers have been successfully studied through the analysis of historical aerial photographs (Roer et al., 2005; Kääb, 2005, 2008; D'Agata and Zanutta, 2007; Diolaiuti et al., 2009; Kaufmann and Ladstädter, 2010; Janke et al., 2013;).

This paper presents a study of changes in the superficial morphology of the Fremri-Grjótárdalur rock glacier and the Hóladalsjökull debris-covered glacier, with the analysis of high-resolution aerial photograph series dating from 1946, 1980, 1985 and 1994 along side the 2000 orthophoto (0.5m spatial resolution), supplied by the National Land Survey of Iceland and the orthophoto supplied by Loftmyndir ehf. The observation therefore covers a period of 54 years, considered sufficient time to detect block movement, which normally does not exceed a few decimeters per year in rock glaciers (Barsch, 1996). More specifically, the photogrammetric techniques and GIS analysis were used to: (i) obtain measurements of horizontal movement and elevation changes of large boulders located on the surface of rock glaciers and debris-covered glaciers; (ii) determine the displacement of the main landforms such as ridges and furrows; (iii) obtain elevation differences by comparing the digital elevation models of 1980 and 1994. To do this, the following steps were required:

4.1 Geomorphological analysis

The first step was to carry out a geomorphological study of each landform by photo interpretation of stereo aerial photographs and fieldwork. The main homogeneous flow units differentiated in each glacier were outlined and mapped, to facilitate their control, description, and interpretation.The active or fossil rock glaciers were considered, with attention to previous publications where appropriate techniques were applied (Andrés et al., 2016; Farbrot et al., 2007; Kellerer-Pirklbauer et al., 2007).

4.2 Creation of stereo-models and uncertainty errors

Overlapping stereo aerial photographs were processed using the commercial Digital Photogrammetric WorkStation Digi3d.NET (DPWS Digi3d) to obtain stereo-models of the area of rock glaciers and the debris-covered glacier for each date considered. Generating the stereo-models involved the geometric correction of the stereo aerial photographs from each date. First, internal orientation was carried out with the help of the camera calibration parameters and additional information appearing in the photo frames (i.e. focal length and fiducial marks). Absolute orientation was then defined based on the accurate identification of a set of 16 geo-referenced ground control points (GCP) on the 2000 orthophoto. GCP were also detected on the aerial photos from the remaining dates. The elevation of each GCP was extracted from the 1:20.000 topographic map. The root mean square error (RMSE) of the absolute geometric correction for each stereo-model in x, y, z (RMSExyz) was very low, between 0.153 and 0.251 m (Table 1). Only the model from 1946 presented a higher RMSExyz because the photo frame is cut and the camera focal length and position of the fiducial marks are unknown.

4.3 Generating orthophotos

In the next phase, orthophotos of the study area for each date were generated, with spatial resolution of 0.25m. These orthophotos provide a first high-precision visual observation of the morphological evolution of these glaciers (see complementary material).

4.4 Photo-interpretation and 3D photogrammetric restitution of surface geomorphological elements

The changes produced on the glacier surfaces were detected through a spatial correlation analysis applied to the multitemporal series of stereo-models. A digital photogrammetric workstation was used for photo interpretation and manual restitution of the main surface features of the glaciers in 3D. The most easily recognizable landforms on the surface were mapped in each stereo-model, including internal transverse and longitudinal ridges and furrows, lateral and frontal crests, thermokarst depressions and large boulders. Each one of these landforms was identified for each date, to analyze their dynamic evolution and horizontal and vertical displacement, according to the following phases:

4.4.1. Quantifying individual block movement

Monitoring large blocks or boulders has frequently been used to measure and quantify rock glacier movement using orthophotos from different dates. This monitoring can be done by manual point-to-point methods (Gorbunov et al., 1992; Janke, 2005; Kääb et al., 1997), by using differential GPS (Bosson and Lambiel, 2016) and by automatic or semi-automatic cross-correlation of multitemporal orthophoto series (Capt et al., 2016; Kääb et al., 2003, 1997; Kaufmann and Ladstädter, 2010; Roer et al., 2005; Roer and Nyenhuis, 2007). This last method allows horizontal displacement vectors to be obtained automatically and enables the measurement and calculation of displacement and velocities of individual blocks.

In this study the manual point-to-point method was used, with some improvements. First, large boulders were identified in the orthophotos by visual inspection using a CAD platform (Bentley MicroStation v8i), to obtain an inventory of boulders with their location. The number of boulders identified was limited by the snow coverage and the photo quality on all dates. Secondly, the digital photogrammetric workstation was used to capture the position and coordinates of the maximum point of each identified boulder, recorded as a data point. In addition to the boulders identified on the glaciers, blocks from external areas considered stable were also recorded, to enhance the accuracy of the results. At this stage, a database was created with positional information (x, y, z coordinates) for each block. In the third step, the boulder displacement identified for the Hóladalsjökull debris-covered glacier was determined for 1980-1994 and for the intervals 1946-1980, 1980-1985, 1985-1994 and 1994-2000.

Blocks at the different dates were correlated using the XY to Line geo-processing tool included in the ArcMap data management tools (Esri ArcGIS 10.3). The horizontal displacement vector between the different dates was obtained for each boulder identified and the elevation difference in the attribute table calculated. Relating these parameters to the period durations enabled the average annual velocity and sinking to be obtained for each boulder. Finally, the velocities (m yr^{-1}) and elevation differences (m) of each boulder were interpolated with the kriging routine to obtain a spatial model of the movement distribution in its horizontal and vertical dimensions.

4.4.2. Obtaining the displacement of the linear geomorphological elements.

Only the front of rock glaciers has been monitored in previous studies (Monnier et al., 2014, 2011; Monnier and Kinnard, 2015a). In this study, the digital photogrammetric workstation was also used for the 3D restitution of the main linear landforms (ridges,

furrows, lateral and frontal crests, limits of depressions) on each stereo-model. Thus, these landforms were mapped for years 1946, 1980, 1985, 1994 and for the 2000 orthophoto. Repeated measurements were then implemented in a CAD throughout each period to obtain the displacement of each landform. This software enables simultaneous working with multiple views and so the position of each feature at each date can be easily identified.

4.5 Digital Elevation Models (DEM)

In previous studies with similar aims to this present study, a Digital Elevation Model (DEM) was generated automatically by applying digital photogrammetry to historical aerial photographs (Capt et al., 2016; D'Agata and Zanutta, 2007; Janke, 2005; Kääb et al., 2003; Wangensteen et al., 2006). Here, DEMs were generated from the contour lines and spot elevation, obtained by manual digital photogrammetric restitution in stereoscopic mode, to achieve a more realistic appearance of the terrain topography. First, restitution of the contour lines at 2 m interval in the study area was carried out for 1980 and 1994. This area included the debris-covered-glacier, the rock glaciers and a ~10m fringe outside the glaciers. A large number of spot elevations were also stereo-plotted (2902 for 1980 and 3046 for 1994), mostly located on the glaciers.

Then, DEMs were produced by generating several Triangular Irregular Networks (TIN) from the contour lines and the set of spot elevations in ArcGis 10.3. Next, each TIN was converted to raster format with cellsize 1 m^2 (Fig. 1C) and changes in surface altitude between the dates were calculated using the raster calculator tool. The results were re-classified as positive, negative, or unchanged (between -0.25m and +0.25m, taking the RMSE into account). A statistical analysis of the area of each geomorphological unit was performed with ArcGIS Zonal statistics tool.

5. Results

Analysis of the data obtained from processing the historical aerial photographs of the debris-covered and rock glaciers revealed the evolution of their landforms, horizontal velocities and the elevation changes of large boulders.

5.1 Geomorphological units

The study area was divided into different units to facilitate control and description (Fig. 2A):

5.1.1. The Hóladalsjökull cirque. There are three types of units in this cirque: the debris-covered glacier, which was divided into units (DCG-1 and DCG-2a, 2b and 2c)

according to the debris-cover surface morphology, and a small rock glacier (RG-3) (Fig. 2A).

a.1) *Debris-covered glacier* (DCG-1).This is the debris-covered glacier tongue, characterized by a >2m-thick debris layer visible in numerous collapse depressions (Fig. 3A). The debris-covered surface slope is less than 5º and extends 2 km from the limit of the spoon-shaped depressions to the snout. The snout is at 900 m a.s.l. and forms a steep wall around 30m high with 30º slope (Fig. 2B). This unit is 1.3 km wide and covers an area of 2.21 km^2. The surface morphology shows ridges and furrows running longitudinally to the flow as the dominant features, reaching up to 1.5 km in length (Fig. 3B and 3C). Some of the furrows have permanent snowcover. In the lower sector, smooth transverse ridges and furrows appear parallel to the glacier front.

a.2) *Glacier spoon-shaped depressions*. There are three depressions at the foot of the cirque headwalls, with almost debris-free ice: eastern (DCG-2a in the tables and figures), central (DCG-2b) and western (DCG-2c). Considering each unit from the lower depression limit to the upper glacier limit, they occupy an area of approximately 2.5 km^2, 66.6% of which is formed by debris-free glacial ice and scattered blocks, with the remaining area covered by a thin layer of sediment. These depressions end 1.4 and 1.6 km from the cirque headwalls and are confined at their lower edge by a series of moraine-like block ridges that overlap the debris forming the rest of the debris-covered glacier.

a.3) *The Hóladalsjökull rock glacier* (RG-3). A small rock glacier (0.29 km^2, 600 m long), is located just to the west of Hóladalsjökull in the same cirque, with its front at 904 m a.s.l.

5.1.2. The Fremri-Grjótárdalur cirque. The surface area of all the Fremri-Grjótárdalur rock glaciers is approximately 0.96 km^2. The Fremri-Grjótárdalur cirque is divided here into six different sectors (Fig. 2A and 2B):

b.1) *Active rock glacier in the western sector* (RGW-4a), consisting of a series of lobes, 300 - 400 m in length, terminating at 950-940 ma.s.l. with steep slopes.

b.2) *Active rock glacier in the central sector* (RGW-4b), up to 1 km long, forming many transverse ridges and furrows reaching 896-922 m a.s.l. (Fig. 3D and 3E).

b.3) *Fossil rock glacier in the central sector* (RGW-4c), located at the front of the previous two rock glaciers, but 500 m longer, extending down to 850 m a.s.l.

b.4) *Active rock glacier in the eastern sector* (RGE-5a), an active tongue-shaped rock glacier, 190 m long, 270 m wide, descending to 1002 m a.s.l.

b.5) *Fossil rock glacier in the eastern sector* (RGE-5b), 250 m long and 280 m wide, descending to 978 m a.s.l.

b.6) *Two small active talus rock glaciers* (RGT 6a and 6b), located just at the foot of the headwall.

5.1.3. External stable areas. Rocky outcrops and erratic boulders considered stable (SG -7a and 7b) external to the debris-covered glacier and rock glaciers, used here as fixed control points to validate changes monitored in the glaciers.

5.2*Visual contrast of the orthophotos*

An in-depth visual inspection of the orthophotos of the Hóladalsjökull debris-covered glacier shows an almost total absence of changes in its superficial morphology over the last 54 years (see commplementary material). The main landforms analyzed on the surface of the debris glacier, (transverse and longitudinal ridges and furrows), remained identical in geometry and morphology. Likewise, the landforms analyzed in the outermost sections of the glacier (lateral and frontal crests) did not undergo morphological changes, and do not present any significant progress in the lateral or frontal limits of the debris-covered glacier. The only changes observed in this glacier are the appearance of new thermokarst depressions. E.g., there is a new depression in the orthophotos from1980 compared to 1946; in addition, the formation of new thermokarst hollows was noted in fieldwork in 2014, 2015 and 2016 (Fig. 3B). The same results were obtained for the rock glaciers from the visual analysis of the orthophotos, with no deformation or new thermokarst depressions observed.

5.3 Surface displacements and elevation changes of large boulders.

A significant number of common boulders (>75) in the debris-covered glacier could be identified in the 1980, 1985 and 1994 orthophotos, whereas only 19 and 51 boulders respectively were identified in the 1946 and 2000 orthophotos. For the rock glaciers, only the photographs from 1980 and 1994 were usable. Taking into account these limitations, the displacement analysis of the debris-covered glacier includes the periods 1946-1980 (19 correlated boulders), 1980-1985 (266 boulders), 1985-1994 (308 boulders) and 1994-2000 (51 boulders) as well as the whole period 1980-1994 (270 boulders). The correlation analysis of the rock glacier boulders only includes 1980-

1994, where 308 boulders were correlated.The boulder elevation changes in the debris-covered glacier and rock glaciers for the 14 years 1980 - 1994 were analyzed.

5.3.1. Data quality and measurement uncertainty.

The results of the horizontal displacement of the points on stable ground near the debris-covered glacier obtain mean values ranging from 0.05 to 0.10 m yr^{-1} for the periods 1980-1985, 1985-1994 and for the whole period 1980-1994, confirming the practical absence of movement (Table 2 and 4). The maximum displacement values obtained on stable ground were 0.10 m yr^{-1} (1980-1985), 0.15 m yr^{-1} (1985-1994) and 0.12 m yr^{-1} (1980-1994). These values were considered as uncertainty in the evaluation of the horizontal mobility of boulders located on the glaciers. When measuring the displacement in stable areas surrounding the rock glaciers (SG-7b) a minor error occurs. The 56 stable points displayed a mean velocity of 0.03 m yr^{-1} and a maximum of 0.08 m yr^{-1}, so that these values evidence complete stability. According to the maximum value for the movement of these points, the uncertaintywas 0.08 m yr^{-1}.On the other hand, the mean value obtained for the elevation changes (1980-1994) from the 22 stable control points in the Hóladalsjökull cirque (SG-7) was -0.20 m (σ = 0.416 m), and from the 56 stable control points in the Fremri-Grjótárdalur cirque (SG-7b) was -0.237 m (σ = 0.311 m). Nevertheless, the uncertainty of *z* is more difficult to estimate, given the quality of the photos and human error, so the elevation uncertaintyis also estimated as the extreme values in the maximum and minimum elevation data obtained from the set of all stable control points. Thus, at some stable points a maximum negative (or dipping) elevation difference was obtained of -0.94m (SG7a and b unities) and a maximum positive of 0.81m (SG-7a) and 0.38 m (SG-7b), so that these extreme values can be considered as the maximum uncertainty of *z* in the block elevation changes (Table 3 and 4).

5.3.2. Horizontal displacement velocity of large boulders in the debris-covered glacier.

The results for horizontal mobility of the 172 boulders for the 1980-1994 period in the debris-covered glacier (DCG-1) obtain a mean velocity of 0.33 m yr^{-1} ranging from less than 0.025 to 1.16 m yr^{-1} (Table 2). The results of interpolating the blockvelocity (Fig. 4A, map 1980-1994) obtain only slight mobility in the central sector of the debris-covered glacier (DCG-1), from the western spoon-shaped hollow to its eastern front, where velocity increases from 0.45 to 0.65 m yr^{-1}. The average horizontal velocity of the 72 identified boulders in the spoon-shaped hollows (DCG-2a, 2b and 2c) is slightly

455 lower (0.30 m yr^{-1}), although the extreme values are higher (0.06 and 1.59 m yr^{-1}
456 respectively). The highest velocity values (>0.7 m yr^{-1}) occur where the debris-covered
457 glacier originates, between the eastern (DCG-2b) and central (DCG-2c) spoon-shaped
458 hollows (Fig.4A, 1980-1994 map). The overall block velocity for the completely debris-
459 covered glacier and the spoon-shaped hollow is <0.5m yr^{-1}.
460 The mobility of the debris-covered glacier (DCG-1) boulders presents very similar
461 horizontal velocities in the intermediate periods: 0.32 m yr^{-1} between 1980 and 1985
462 and 0.35 m yr^{-1} between 1985 and 1994 (Fig. 5A). Similarly, mobility at the spoon-
463 shaped depressions (DCG-2a, 2b and 2c) yields practically identical values in 1980-
464 1985 (0.30 m yr^{-1}) and in 1985-1994 (0.32 m yr^{-1}). Therefore, the average velocity
465 range is 0.33 m yr^{-1} for the whole 14-year interval. The spatial movement distribution
466 shows that the greatest displacement in the debris-covered glacier occurs in a small
467 sector at the northeastern edge of the front, where horizontal velocities reached between
468 0.6 and 0.7 m yr^{-1}. The rest of the debris-covered surface remained with displacement
469 rates lower than 0.5 m yr^{-1}, but with broad sectors as low as 0.35 m yr^{-1}. Finally,
470 although the number of boulders identified is very limited, the horizontal displacement
471 values obtained for the periods 1946-1980 and 1994-2000 yield mean velocities of 0.30
472 m yr^{-1} and 0.25 m yr^{-1} respectively. The results, therefore, reflect values similar to
473 those obtained in the other periods analyzed.
474 *5.3.3. Elevation changes of large boulders in the debris-covered glacier.*
475 The elevation changes of the 172 boulders identified on the surface of the debris-
476 covered glacier (DWG-1) during the period 1980-1994 reflect an average sinking of -
477 0.72 m, with this value increasing up to -1.14 m in the 72 boulders of the spoon-shaped
478 depressions (DCG-2 a, 2b and 2c). The maximum negative values recorded are -2.78
479 and -3.11 m respectively (Table 3). Approximately 90% of the measured boulders yield
480 negative values, indicating a tendency to surface lowering during the 14 years (Fig. 4B).
481 However, as can be seen on the map, some sectors of the DCG-1 unit show losses
482 greater than a meter in ice thickness, in an area that coincides with the formation of
483 thermokarst collapse depressions observed in the field (Fig. 3A). Another area with
484 greater surface lowering is the debris-covered glacier front, in both its western sector
485 and especially at its eastern edge, which coincides with the area where the horizontal
486 displacements are greatest (Fig. 5A and 5B). The spoon-shaped hollows, at the limit of

clean ice, present greater subsidence, seen especially in the western depression (DCG-2c), with more than 1.5-2m of total sinking the period 1946-2000.

5.3.4 Displacement velocities and elevation changes of large boulders in the rock glaciers.

231 boulders were correlated in the Fremri-Grjótárdalur cirque rock glacier, and 21 in the small rock glacier of the Hóladalsjökull cirque. The results reflect a displacement rate of less than 0.15 m yr^{-1} in 14 years (1980-1994) (Table 4 and Fig. 4A). The mobility only increases slightly in the two upper west lobes (RGW-4b), just in the transverse crests with abrupt fronts (0.29 and 0.23 m yr^{-1}). The lower western rock glacier (RGW-4c) yields results confirming its fossil character since all the measured boulders show a velocity inferior to 0.1 m yr^{-1}. The eastern rock glaciers present very low rates: 0.04 m yr^{-1} in the upper lobe (RGE-5a) and 0.02 m yr^{-1} in the lower lobe (RGE-2b). The talus-derived rock glaciers (RGT-6a and 6b) show displacement of less than 0.05 m yr^{-1}. Finally, the small rock glacier (RG-3), located southwest of the Hóladalsjökull debris-covered glacier, displays absence of horizontal movement, with velocities lower than 0.1 m yr^{-1} (0.034 m yr^{-1} on average). To sum up, the measurements of the horizontal displacements in rock glaciers indicate that they are motionless with rates below the margin of error.

For changes of block elevation over14 years (1980 - 1994), the Fremri-Grjótárdalur rock glaciers yield an average value of -0.37 m, whereas the value for the Hóladalsjökull rock glacier is -0.24 m, indicating a trend to subsidence (Table 4 and Fig. 4B).

5.4. Surface changes in linear geomorphological features: ridges and furrows.

Contrasting the geomorphological maps (Fig. 6A and 6B) from various years enabled the measurement of linear landform displacement over 54 years (1946-2000) for the debris-covered glacier and 14 years (1980-1994) for this same glacier and for the rock glaciers.

5.4.1. Surface changes in linear geomorphological features in the debris-covered glacier.

In the case of the debris-covered glacier, 10 ridges and 8 furrows in the 1946-2000 period, and 17 ridges and 16 furrows in 1980-1994 were identified and digitized in 3D stereo mode to calculate their displacement rates (Fig.6A and Table 5). These landforms

are mainly located in the frontal, central and eastern sectors. The results show that the ridges and the furrows experienced an advance of 14.87m and 13.05 m respectively during the 1946-2000 period, representing rates of 0.27 m yr^{-1} and 0.24 m yr^{-1}, respectively (Table 5). In 1980-1994, the average displacement rate of the ridges was appreciably reduced: 0.226m yr^{-1} (3.17m in 14 years). The reduced advance of these landforms is most likely related to a surface lowering process, since these lines show an average elevation decrease of 0.6 m (0.04 m yr^{-1}). The sector of the debris-covered glacier that shows the greatest sinking is at the southeastern border and coincides exactly with the area where the boulders show the greatest movement. On the contrary, the lines that define the fronts and lateral ridges of the eastern and western parts of the debris-covered glacier remained practically immobile (Fig. 6B). In fact, only the transverse furrows show movement, whereas most of the longitudinal furrows have remained static.

In conclusion, the slow dynamics of the debris-covered glacier over the 54 years may be related to certain amount of sinking and did not change its surface morphology, except for the formation of some depressions due to collapse.

5.4.2. Surface changes in linear geomorphological features of the rock glaciers.

The results obtained in the rock glaciers indicate the almost total absence of displacement of the linear landforms (Fig.6A). Only slight displacements were observed in 10 ridges and 15 transverse furrows in the upper and central west lobes (RGW-4a and 4b) for the period 1980-1994, with velocity 0.10 m yr^{-1}, and elevation difference -0.39 m (Table 6).

5.5. Surface elevation changes from DEM: 1980-1994.

When calculating the differences in surface elevation of the debris-covered glacier and the rock glaciers derived from comparing high resolution DEMs between 1980 and 1994, but the results are affected by the heavy snow coverage in the 1994 photograph. This means many of the volume changes are positive, especially in the numerous longitudinal and transverse furrows of the glaciers. We rejected the areas with positive volume changes from 1980 to 1994 in our analysis, considering that these positive values were due to the importance of the snow cover in 1994 (Table 7 and Fig. 7). According with our results, considering only the 55% of the surface of the debris-

553 covered glacier (DCG-1), show around 294,510 m^3 volume losing a 20% of its total
554 area and a mean thinning of 0.69 m. This value is very similar to that obtained when
555 comparing the elevation differences between the boulders (-0.72 m). In addition, we
556 will able to consider the 55% of the surface of the spoon-shaped depression area (DCG-
557 2 a, 2b and 2c) which also yields negative values in the 35% of its total area, with a loss
558 of 286,703 m^3 and average thinning of 0.97 m. The results for the Fremri-Grjotárdalur
559 rock glaciers as a whole, considering the 50% of the area, where 20% of its total area
560 has negative values, indicate a volume loss of 191,187 m^3 and average thinning of 0.69
561 m.
562
563 **6. Discussion**
564 To differentiate debris-covered and rock glaciers in Tröllaskagi, debris/ice ratio criteria
565 (Azócar and Brenning, 2010; Brenning, 2005; Haeberli et al., 2006; Hambrey et al.,
566 2008; Kirkbride, 2011, 2000) were applied, with this ratio obtained from the results of
567 previous research (Kellerer-Pirklbauer et al., 2007; Wangensteen et al., 2006) and our
568 field observations on the walls of collapse depressions. Surface morphology criteria for
569 differentiating the two features (Berthling, 2011; Clark et al., 1994; Haeberli et al.,
570 2006; Janke et al., 2013; Monnier and Kinnard, 2017) were also applied. Discriminating
571 between debris-covered and rock glaciers has been a keyfactor in this research as each
572 type of feature currently displays very different dynamics:
573 *6.1. Dynamics of the Hóladalsjökull debris-covered glacier.*
574 Wangensteen et al. (2006) studied the dynamics of the Hóladalsjökull debris-covered
575 glacier applying automatic digital photogrammetry. Their results propose mean
576 velocities of 0.37 m yr^{-1} and a maximum velocity of 0.84 m yr^{-1} from 1985 to 1994. Our
577 study reports a similar mean velocity rate (0.33 m yr^{-1}) for the same period, but a much
578 lower maximum rate (0.65 m yr^{-1}). The areas where maximum displacement rates were
579 recorded in the two studies are in the center and on the eastern edge of the glacier.
580 These areas coincide with the highest slope and the formation of a drainage network on
581 the glacier surface, descending from the spoon-shaped depression to the front. A
582 possible explanation of this coincidence links displacement and greater mobility of the
583 glacier, resulting from the incisive effect of the drainage network.

To complete our analysis of the debris-covered glacier dynamics, the boulder elevation changes in these features was studied here for the first time. High sink values were obtained, with a mean decrease of 0.72 m and maximum values of up to 3.11 m for the period 1980-1994. The subsidence affected most of the boulders and was more intense in the central and eastern sector, precisely where horizontal displacement rates were greater. Sinking was also very intense in sectors where collapse depressions were observed.

Our detailed observation of landforms in orthophotos from 1946 to 2000 shows little or no change, except for some thermokarst collapse depressions. Similarly, according to their observations of the DTM and orthophotos, Wangensteen et al. (2006) recognized the stable geometry and frontal position of all the landforms, despite the evident glacial flow. However, if we apply the speeds deduced by Wangensteen et al., 2006, the fronts would have advanced 20-45 m in the 54 year period (1946-2000). In contrast, our results obtain the maximum advance of the glacier fronts at around 15 m in the same period (1946-2000). During the period 1980-1994, the advance was only about 3 m. If the average sinking 0.6 m of the ridges in the same period is taken into account, the small advance may simply be related to the sinking of the crest on an inclined plane, in response to the slight degradation of an immobile ice mass. This movement would be negligible in an active debris-covered glacier (Bosson and Lambiel, 2016). The frequent formation of collapsed hollows would confirm the melting of buried ice (Emmer et al., 2015). Displacement of the blocks and ridges and their subsidence is only significant in the central and eastern sectors, and most of the limits of the debris-covered glacier remained static for more than fifty years. The tendency to sink affected not only a series of blocks, but is also widespread throughout the glacier surface, with a demonstrated loss of almost 300,000 m^3 in the period 1980-1994 for only 20% of the area that was not covered by seasonal snow.

In conclusion, the boulder displacement observed seems to announce the terminal phase of the glacier, trending to widespread subsidence, more intense where the slope is higher, the onset of a drainage network on its surface and frequent collapse depressions. All these factors reveal the predominantly erosive action of the subglacial channels (Janke et al., 2015; Monnier and Kinnard, 2017) and demonstrate the complete stability of the front and stagnation of the entire ablation area.

The transformation of debris-free glaciers into debris-covered glaciers is considered a typical process of a glacial recension stage, where paraglacial processes are accelerated, such as subsequent decompression when the slopes are free of ice (Janke et al., 2015; Monnier and Kinnard, 2017). This transformation can occur over just a few decades (Ackert, 1998; Bosson and Lambiel, 2016; Emmer et al., 2015; Monnier et al., 2011). In some regions, the new debris-covered glaciers display intense dynamics, as e.g. in Patagonia (Glasser et al., 2016). However, in others they tend to stabilize, as e.g. in the Himalayas (Benn et al., 2012; Hambrey et al., 2008) or the Andes (Emmer et al., 2015), where surface lowering and stagnation trends are very similar to Hóladalsjökull. The low intensity of the glacial flow is considered the main cause of the transformation from a debris-covered to a rock glacier in some cases in the Himalayas (Shroder et al., 2000), the Rockies (Ackert, 1998), the Andes (Emmer et al., 2015) and the Alps (Capt et al., 2016). This very different reaction in the development of debris-covered glaciers may respond to regional climatic differences or express different phases within a common paraglacial process (Glasser et al., 2016). In the debris-covered glaciers undergoing stabilization in the regions mentioned above, such as the Himalayas, a trend can be observed from substantial activity to paralysis and stagnation of the glacial fronts over a few decades (Benn et al., 2012; Hambrey et al., 2008). The same occurs in some glaciers in the Alps (Capt et al., 2016) and the Andes (Emmer et al., 2015). However, in the rock glaciers and debris-covered glacier in the Tröllaskagi peninsula, the stagnation of the fronts is evident and permanent over decades. The Hóladalsjökull debris-covered glacier has not changed its superficial morphology in any way from 1946 to the present, except for the appearance of collapse depressions. These depressions do not deform over time. Nevertheless, the surface changes are intense in other debris-covered glaciers in many different regions which maintain some flow dynamics (Benn et al., 2012; Deline, 2005; Hambrey et al., 2008; Janke et al., 2015; Glasser et al., 2016; Monnier and Kinnard, 2017; Anderson et al., 2018; and many other authors). In fact, the absence of morphological changes in Hóladalsjökull is new in the literature on debris-covered glaciers and demonstrates its relict state. This would be facilitated by remaining under permafrost conditions, previously only applicable to rock glaciers (Capt et al., 2016; Monnier and Kinnard, 2015b; Seppi et al., 2015; Shroder et al., 2000).

6.2. Dynamics of rock glaciers in the Hóladalsjökull and Fremri-Grjótárdalur cirques.

The results of previous studies of rock glaciers (Kellerer-Pirklbauer et al., 2007; Wangensteen et al., 2006) completely differ from those obtained in this study. These authors obtain velocity rates between 0.11 m yr^{-1} and 0.79 m yr^{-1} for the period 1985-1994, very similar to those of the debris-covered glacier. In contrast, the results of our work here show that these glaciers are practically static, with displacements less than 0.15 m yr^{-1} in 14 years (1980-1994), below the calculated rate of uncertainty. The results of Lilleøren et al. (2013) diverge even more from ours, as they observed up to 3 m horizontal displacements in a few months. However, our results indicate that the rock glacier horizontal movement is insignificant, but the block collapse is not, with values between 0.24 and 0.37 m in a 14-year period. The analysis of ridge displacement in rock glaciers also shows their static nature, with a maximum movement of only 5 m in 48 years. Our results agree more closely with those obtained in the Nautárdalur rock glacier (Martin and Whalley, 1987; Whalley and Martin, 1994) by geodetic techniques (theodolite) and direct observation methods. These authors obtained velocity ratios of 0.25 m yr^{-1} for a period of 17 years (1977-1994) in some rock glacier boulders but consider the glacier virtually static as a whole with its front advancing less than 1 m in that period. In short, photogrammetric data and observations at different dates show that flow in these rock glaciers is non-existent, despite the presence of interstitial ice and the total conservation of their surface landforms over time. The only activity is a tendency to subsidence and volume loss, also evident in a certain horizontal displacement, as they are located on an inclined plane. In fact, the ratio between horizontal and vertical displacement is very different from that obtained in any active rock glaciers (Bosson and Lambiel, 2016; Janke, 2005), since subsidence in Tröllaskagi is proportionally much greater in relation to the horizontal displacement, as has also been observed in other rock glaciers in a total stabilization process (Dusik et al., 2015).

The type and intensity of the flow is the origin of the rock glacier surface morphology (Janke et al., 2015, 2013). The rock glaciers studied here in Tröllaskagi display a very varied morphology, showing different phases of flow intensity. Nevertheless, once the rock glaciers lost their dynamism, these landforms were more easily conserved. Even the steep frontal slopes, considered an indicator of their capacity to advance (Janke et al., 2015, 2013), remain totally immobile for decades, as has been reported in similar cases (Emmer et al., 2015).

6.3. Relationship between the dynamics of the debris-covered and rock glaciers and climate change.

In both the debris-covered glacier and the rock glaciers their subsidence process would be attenuated to be above the permafrost level (Capt et al., 2016; Etzelmüller et al., 2007; Monnier and Kinnard, 2015b; Seppi et al., 2015; Shroder et al., 2000; Wangensteen et al., 2006). But, in fact, these glaciers would be just at the altitudinal limit of permafrost according to models derived from the meteorological series of recent decades (Etzelmüller et al., 2007; Kellerer-Pirklbauer et al., 2007). In turn, regional warming, and therefore the corresponding rise in the permafrost level, is evident from the LIA (Caseldine and Stötter, 1993) and has been accentuated in recent decades (Fernández-Fernández et al., 2017). The predominant subsidence dynamics of these formations could be considered related to permafrost degradation. In several examples in the Alps, an increase in temperature increases the flow velocity of rock glaciers (Delaloye et al., 2008; Kellerer-Pirklbauer and Kaufmann, 2012; Kellerer-Pirklbauer et al., 2008; Roer et al., 2005; Wirz et al., 2016; Kääb et al., 2003; Roer et al., 2005; Kellerer-Pirklbauer et al., 2017; among others). However, the rock glaciers in Tröllaskagi remain with practically no horizontal displacement, despite the increase in temperature. This difference in behavior may, in the case of Tröllaskagi, be due to the fact that these formations are based on valley bottoms with very little slope. In the Alps it has been shown that two rock glaciers in close proximity can have a very different responses to climate change, according to their local topographic characteristics (Bosson and Lambiel, 2016). The velocity of debris-covered and rock glaciers is related not only to the effects of warming, which increase ablation, but also to the amount of debris contributed to the system, which reduces ablation (Anderson and Anderson, 2016). On the other hand, the amount of debris contributed depends on the climate, and on many other factors, such as local topography, tectonic setting, geomorphological evolution, etc., which greatly complicate the calculation of the relationship between climate change and rock glacier flow (Gibson et al., 2017). The mobility of debris-covered glaciers and rock glaciers depends more on the amount of water supplied to the system, which in turn is not directly proportionally related to the increase in air temperature (Bodin et al., 2009; Kenner et al., 2017).

In any case, rock glaciers in Tröllaskagi and the Alps, despite the different behavior of their horizontal displacement, maintain a constant tendency to subsidence (Barsch,

713 1996; Capt et al., 2016; Kääb, 2008; Kellerer-Pirklbauer and Kaufmann, 2012; Kellerer-
714 Pirklbauer et al., 2008; among others).

715 The extraordinary sensitivity to temperature changes observed in the debris-free glaciers
716 on Tröllaskagi (Fernández-Fernández et al., 2017), with intense, rapid advances and
717 retreats over recent decades, is not reflected at all in debris-covered and rock glaciers
718 located in coalescent cirques, where the slow tendency to degradation is neither
719 accelerated nor interrupted by these thermal changes. This contradicts what has been
720 observed in other regions, such as e.g. Patagonia (Glasser et al., 2016), the Himalayas
721 (Benn et al., 2012; Hambrey et al., 2008), Alaska (Pelto et al., 2013), or the Alps
722 (Kellerer-Pirklbauer and Kaufmann, 2012), especially in relation to debris-covered
723 glaciers, where their reaction to climate changes seems to be instantaneous. In other
724 cases, such as in the Rocky Mountains, rock glaciers have maintained an unchanging
725 flow for decades (Janke, 2005; Janke et al., 2013; Potter et al.,1998). The lack of
726 climatic sensitivity of the rock glaciers and in particular of the debris-covered glacier in
727 Tröllaskagi, may be because they originated in very different climatic situations from
728 the present day and were preserved in time only in static form.

729 *6.4. Relationship between the dynamics of the debris-covered and rock glaciers and*
730 *their ages and origin*.

731 According to our results, we cannot confirm how long the debris-covered and rock
732 glaciers in Tröllaskagi have remained in a state of permanent subsidence and stagnation
733 without any real flow. For this reason, it makes no sense to extrapolate the current
734 situation in Tröllaskagi and in other mountain areas, to deduce the origin and formation
735 date of the debris-covered and rock glaciers, as inferred in many previous studies
736 (Ackert, 1998; Farbrot et al., 2007; Hamilton and Whalley, 1995a, 1995b; Kellerer-
737 Pirklbauer et al., 2007; Lilleøren et al., 2013; Martin and Whalley, 1987; Martin et al.,
738 1991; Wangensteen et al., 2006; Whalley and Martin, 1994). This type of stagnation
739 period may have been repeated throughout the history of the rock and debris-covered
740 glaciers, and therefore this non-linearity strongly reduces the applicability of this
741 approach.

742 *6.5. Degree of uncertainty in automatic and manual methods.*

743 There is clearly a degree of uncertainty when analyzing historical aerial photographs
744 using digital photogrammetry. This is dependent on the quality of the photos, their

745 contrast, the presence of shading, snow, etc. In this case, the degree of uncertainty has
746 been reduced by manually restitution each geomorphological element in 3D (large
747 boulders, crest and furrows) for each stereo-model. On the contrary, automatic cross-
748 correlation techniques are currently preferred, matching homologous points in two
749 orthophotos (Avian et al., 2005; Dall'Asta et al., 2017; Kaufmann and Ladstädter, 2010;
750 Wangensteen et al., 2006).

751 In addition, as a result of the restitution of stable landforms outside the glaciers, we
752 obtained a good indicator of the accuracy of the computed mean annual flow velocity
753 and elevation changes (Avian et al., 2005; Janke, 2005; Monnier and Kinnard, 2017).

754 The application of digital photogrammetry using automatic orthophoto correlation, as
755 previously applied in Tröllaskagi, tends to overestimate surface displacement values in
756 debris-covered glaciers and particularly in rock glaciers. If the velocities proposed
757 previously by other authors (Kellerer-Pirklbauer et al., 2007; Wangensteen et al., 2006),
758 close to 1 m yr^{-1} were real, this would be seen in a change in surface morphology. This
759 change has not been detected in Tröllaskagi, but is seen in rock glaciers in the Alps,
760 where the application of automatic digital photogrammetry techniques to historical
761 photographs reflects important geomorphological modifications on rock glacier surfaces
762 (Avian et al., 2005; Kääb, 2002; Kaufmann and Ladstädter, 2010, 2003; Roer et al.,
763 2005).

764 **7. Conclusions**

765 The combination of manual and traditional methods for analysis of the dynamics of
766 debris-covered glaciers and rock glaciers, used with automatic digital methods, has
767 proved to be an effective tool when analyzing long periods, using existing aerial
768 photographs from the 1940s to the present. In addition, the precision of the results is
769 considerably enhanced compared to using only digital and automatic methods. The
770 slight or null movement is translated from a geomorphological point of view into the
771 conservation and stability of detailed forms, where the transverse and longitudinal crests
772 and furrows continue to maintain practically the same position and morphology. The
773 main dynamics of the Hóladalsjökull debris-covered glacier and Fremri Grjótárdalur
774 rock glaciers in the Tröllaskagi peninsula are almost exclusively related to subsidence
775 processes and both formations behave like bodies of stagnation ice. They are insensitive
776 to the contrast between periods of very different temperature. The dynamics of the

debris-covered glacier are not related to climate evolution, although the debris-free glaciers nearby react almost immediately to minimal variations in air temperature over a few years.

The debris-covered and rock glaciers in Tröllaskagi have landforms generated in periods of great dynamism, although at present this is minimal or null. For this reason, their origin and age cannot be deduced from their current dynamics, as many previous studies have attempted to do. On the contrary, their current behavior seems to indicate that they are formations originating under climatic conditions very different from the current ones. Ice survives in the interior of the glaciers when permafrost conditions pertain, although the global warming of recent decades is modifying these conditions. Our results highlight the application of automatic methods for rock glacier monitoring, which greatly simplify the work of researchers, but which may overestimate the results and reach erroneous conclusions.

Acknowledgements

This paper was funded by Project CGL2015-65813-R, (Spanish Ministry of Economy and Competitiveness), Nils Mobility Program (EEA GRANTS) and with the help of the High Mountain Physical Geography Research Group (Complutense University Madrid). The authors would like to thank the Icelandic Institute of Natural History and Hólar University College for their support in the field. We appreciate the important suggestions made by two anonymous reviewers, and their application has significantly improved the manuscript.

References

Ackert, R.P.J., 1998. A rock glacier/debris-covered glacier system at Galena Creek, Absaroka Mountains, Wyoming. Geogr. Ann. Ser. A, Phys. Geogr. 80, 267–276. https://doi.org/10.1111/j.0435-3676.1998.00042.x.

Anderson, L.S., Anderson, R.S., 2016. Modeling debris-covered glaciers: response to steady debris deposition. Cryosphere 10, 1105–1124. https://doi.org/10.5194/tc-10-1105- 2016.

Anderson, R.S., Anderson, L.S., Armstrong, W.H., Rossi, M.W., Crump, S.E., 2018. Glaciation of alpine valleys: the glacier – debris-covered glacier – rock glacier continuum. Geomorphology 311, 127–142. https://doi.org/10.1016/j.geomorph.2018.03.015.

Andrés, N., Tanarro, L.M., Fernández, J.M., Palacios, D., 2016. The origin of glacial alpine landscape in Tröllaskagi Peninsula (North Iceland). Cuad. Investig. Geográfica 42, 341–368. https://doi.org/10.18172/cig.2935.

Avian, M., Kaufmann, V., Lieb, G.K., 2005. Recent and Holocene dynamics of a rock glacier system: the example of Langtalkar (Central Alps, Austria). Nor. Geol. Tidsskr. 59, 149–156. https://doi.org/10.1080/00291950510020637.

Azócar, G.F., Brenning, A., 2010. Hydrological and geomorphological significance of rock glaciers in the dry Andes, Chile (27°–33°S). Permafr. Periglac. Process. 21, 42–53. https://doi.org/10.1002/ppp.669.

Barsch, D., 1992. Permafrost creep and rockglaciers. Permafr. Periglac. Process. 3, 175–188. https://doi.org/10.1002/ppp.3430030303.

Barsch, D., 1996. Rockglaciers, Springer Series in Physical Environment. Springer Berlin Heidelberg, Berlin, Heidelberg https://doi.org/10.1007/978-3-642-80093-1.

Benn, D.I., Bolch, T., Hands, K., Gulley, J., Luckman, A., Nicholson, L.I., Quincey, D., Thompson, S., Toumi, R., Wiseman, S., 2012. Response of debris-covered glaciers in the Mount Everest region to recent warming, and implications for outburst flood hazards. Earth Sci. Rev. 114, 156–174. https://doi.org/10.1016/j.earscirev.2012.03.008.

Berthling, I., 2011. Beyond confusion: Rock glaciers as cryo-conditioned landforms. Geomorphology 131, 98–106. https://doi.org/10.1016/j.geomorph.2011.05.002.

Björnsson, H., 1991. Jöklar á Tröllaskaga. In: Hjálmarsson, Angantýr H. (Ed.), Fjalllendi Eyjafjarðar að vestanverðu II. Árbók Ferðafélags Íslands, pp. 21–37.

Björnsson, H., Pálsson, F., 2008. Icelandic glaciers. Jökull 58, 365–386.

Björnsson, H., Pálsson, F., Sigurðsson, O., Flowers, G.E., 2003. Surges of glaciers in Iceland. Ann. Glaciol. 36, 82–89.

Bodin, X., Thibert, E., Fabre, D., Ribolini, A., Schoeneich, P., Francou, B., Reynaud, L., Fort, M., 2009. Two decades of responses (1986–2006) to climate by the Laurichard rock glacier, French Alps. Permafr. Periglac. Process. 20, 331–344. https://doi.org/10.1002/ppp.665.

Bosson, J.-B., Lambiel, C., 2016. Internal structure and current evolution of very small debris-covered glacier systems located in alpine permafrost environments. Front. Earth Sci., 4 https://doi.org/10.3389/feart.2016.00039.

Brenning, A., 2005. Geomorphological, hydrological and climatic significance of rock glaciers in the Andes of Central Chile (33–35°S). Permafr. Periglac. Process. 16, 231–240. https://doi.org/10.1002/ppp.528.

Brynjólfsson, S., Ingólfsson, Ó., Schomacker, A., 2012. Surge fingerprinting of cirque glaciers at the Tröllaskagi peninsula, North Iceland. Jökull 62, 153–168.

Capps, S.R., 1910. Rock glaciers in Alaska. J. Geol. 18, 359–375.

Capt, M., Bosson, J.B.B., Fischer, M., Micheletti, N., Lambiel, C., 2016. Decadal evolution of a very small heavily debris-covered glacier in an Alpine permafrost environment. J. Glaciol. 62, 535–551. https://doi.org/10.1017/jog.2016.56.

Caseldine, C., 1983. Resurvey of the margins of Gljufurarjokull and the chronology of recent deglaciation. Jökull 33, 111–118.

Caseldine, C.J., 1985. The extent of some glaciers in northern Iceland during the little ice age and the nature of recent deglaciation. Geogr. J. 151, 215–227. https://doi.org/10.2307/633535.

Caseldine, C., Stötter, J., 1993. "Little Ice Age" glaciation of Tröllaskagi peninsula, northern Iceland: climatic implications for reconstructed equilibrium line altitudes (ELAS). The Holocene 3, 357–366. https://doi.org/10.1177/095968369300300408.

Clark, D.H., Clark, M.M., Gillespie, A.R., 1994. Debris-covered glaciers in the Sierra Nevada, California, and their implications for snowline reconstructions. Quat. Res. 41, 139–153. https://doi.org/10.1006/qres.1994.1016.

Coquin, J., Mercier, D., Bourgeois, O., Cossart, E., Decaulne, A., 2015. Gravitational spreading of mountain ridges coeval with Late Weichselian deglaciation: Impact on glacial landscapes in Tröllaskagi, northern Iceland. Quat. Sci. Rev. 107, 197–213. https://doi.org/10.1016/j.quascirev.2014.10.023.

Cossart, E., Mercier, D., Decaulne, A., Feuillet, T., Jónsson, H.P., Saemundsson, Þ., 2014. Impacts of post-glacial rebound on landslide spatial distribution at a regional scale in northern Iceland (Skagafjörður). Earth Surf. Process. Landf. 39, 336–350. https://doi.org/10.1002/esp.3450.

Crochet, P., Jóhannesson, T., Jónsson, T., Sigurðsson, O., Björnsson, H., Pálsson, F., Barstad, I., 2007. Estimating the spatial distribution of precipitation in iceland using a linear model of orographic precipitation. J. Hydrometeorol. 8, 1285–1306. https://doi.org/10.1175/2007JHM795.1.

D'Agata, C., Zanutta, A., 2007. Reconstruction of the recent changes of a debris-covered glacier (Brenva Glacier, Mont Blanc Massif, Italy) using indirect sources: methods, results and validation. Glob. Planet. Chang. 56, 57–68. https://doi.org/10.1016/J.GLOPLACHA.2006.07.021.

Dall'Asta, E., Forlani, G., Roncella, R., Santise, M., Diotri, F., Morra Di Cella, U., 2017. Unmanned Aerial Systems and DSM matching for rock glacier monitoring. ISPRS J. Photogramm. Remote Sens. 127, 102–114. https://doi.org/10.1016/j.isprsjprs.2016.10.003.

Delaloye, R., Perruchoud, E., Avian, M., Kaufmann, V., Bodin, X., Hausmann, H., Ikeda, A., Kääb, A., Kellerer-Pirklbauer, A., Krainer, K., Lambiel, C., Mihajlovic, D., Staub, B., Roer, I., Thibert, E., 2008. Recent interannual variations of rock glacier creep in the European Alps. Ninth International Conference on Permafrost. Fairbanks, Alaska,United States, pp. 343–348.

Deline, P., 2005. Change in surface debris cover on Mont Blanc massif glaciers after the"Little Ice Age" termination. The Holocene 15, 302–309. https://doi.org/10.1191/0959683605hl809rr.

Diolaiuti, G., D'Agata, C., Meazza, A., Zanutta, A., Smiraglia, C., 2009. Recent (1975–2003) changes in the Miage debris-covered glacier tongue (Mont Blanc, Italy) from analysis of aerial photos and maps. Geografia Fisica E Dinamica Quaternaria, pp. 117–127.

Dusik, J.-M., Leopold, M., Heckmann, T., Haas, F., Hilger, L., Morche, D., Neugirg, F., Becht, M., 2015. Influence of glacier advance on the development of the multipart Riffeltal rock glacier, Central Austrian Alps. Earth Surf. Process. Landf. 40, 965–980. https://doi.org/10.1002/esp.3695.

Emmer, A., Loarte, E.C., Klimeš, J., Vilímek, V., 2015. Recent evolution and degradation of the bent Jatunraju glacier (Cordillera Blanca, Peru). Geomorphology 228, 345–355. https://doi.org/10.1016/J.GEOMORPH.2014.09.018.

Etzelmüller, B., Farbrot, H., Guðmundsson, Á., Humlum, O., Tveito, O.E., Björnsson, H., 2007. The regional distribution of mountain permafrost in Iceland. Permafr. Periglac. Process. 18, 185–199. https://doi.org/10.1002/ppp.583.

Eyþórsson, J., 1931. On the present position of the glaciers in Iceland: some preliminary studies and investigations in the summer 1930. Vísindafélag íslendinga 10, 1–35.

Eyþórsson, J., 1935. On the variations of glaciers in Iceland. Some studies made in 1931. Geogr. Ann. 17, 121–137. https://doi.org/10.2307/519954.

Farbrot, H., Etzelmüller, B., Guðmundsson, Á., Humlum, O., Kellerer-Pirklbauer, A., Eiken, T., Wangensteen, B., 2007. Rock glaciers and permafrost in Tröllaskagi, northern Iceland. Z. Geomorph. N.F. (Suppl. 51), 1–16 https://doi.org/10.1127/0372-8854/2007/0051S2-0001.

Fernández-Fernández, J.M., Andrés, N., Sæmundsson, Þ., Brynjólfsson, S., Palacios, D., 2017. High sensitivity of North Iceland (Tröllaskagi) debris-free glaciers to climatic change from the "Little Ice Age" to the present. The Holocene 27, 1187–1200. https://doi.org/10.1177/0959683616683262.

Feuillet, T., Coquin, J., Mercier, D., Cossart, E., Decaulne, A., Jónsson, H.P., Sæmundsson, Þ., 2014. Focusing on the spatial non-stationarity of landslide predisposing factors in northern Iceland. Prog. Phys. Geogr. 38, 354–377. https://doi.org/10.1177/0309133314528944.

Geirsdóttir, Á., 2011. Pliocene and pleistocene glaciations of Iceland. Developments in Quaternary Science. Elsevier, pp. 199–210 https://doi.org/10.1016/B978-0-444-53447-7.00016-7.

Geirsdóttir, Á., Miller, G.H., Axford, Y., Ólafsdóttir, Sædís, 2009. Holocene and latest Pleistocene climate and glacier fluctuations in Iceland. Quat. Sci. Rev. 28, 2107–2118.https://doi.org/10.1016/j.quascirev.2009.03.013.

Gibson, M.J., Glasser, N.F., Quincey, D.J., Rowan, A.V., Irvine-Fynn, T.D., 2017. Changes in glacier surface cover on Baltoro glacier, Karakoram, north Pakistan, 2001–2012. J. Maps 13, 100–108. https://doi.org/10.1080/17445647.2016.1264319.

Glasser, N.F., Jansson, K.N., Duller, G.A.T., Singarayer, J., Holloway, M., Harrison, S., 2016. Glacial lake drainage in Patagonia (13–8 kyr) and response of the adjacent Pacific Ocean. Sci. Rep. 6, 21064.

Gorbunov, A.P., Titkov, S.N., Polyakov, V.G., 1992. Dynamics of rock glaciers of the Northern Tien Shan and the Djungar Ala Tau, Kazakhstan. Permafr. Periglac. Process. 3, 29–39. https://doi.org/10.1002/ppp.3430030105.

Haeberli, W., Hallet, B., Arenson, L., Elconin, R., Humlum, O., Kääb, A., Kaufmann, V., Ladanyi, B., Matsuoka, N., Springman, S., Mühll, D.V., 2006. Permafrost creep androck glacier dynamics. Permafr. Periglac. Process. 17, 189–214. https://doi.org/10.1002/ppp.561.

Hambrey, M.J., Quincey, D.J., Glasser, N.F., Reynolds, J.M., Richardson, S.J., Clemmens, S., 2008. Sedimentological, geomorphological and dynamic context of

942 debris-mantled glaciers, Mount Everest (Sagarmatha) region, Nepal. Quat. Sci. Rev.
943 27, 2361–2389. https://doi.org/10.1016/j.quascirev.2008.08.010.

944 Hamilton, S.J., Whalley, W.B., 1995a. Preliminary results from the lichenometric
945 study of the Nautardálur rock glacier, Tröllaskagi, northern Iceland. Geomorphology
946 12, 123–132. https://doi.org/10.1016/0169-555X(94)00083-4.

947 Hamilton, S.J., Whalley, W.B., 1995b. Rock glacier nomenclature: a re-assessment.
948 Geomorphology 14, 73–80. https://doi.org/10.1016/0169-555X(95)00036-5.

949 Humlum, O., 1998. The climatic significance of rock glaciers. Permafr. Periglac.
950 Process. 9, 375–395. https://doi.org/10.1002/(SICI)1099-
951 1530(199810/12)9:4b375::AIDPPP301N3.0.CO;2-0.

952 Icelandic Meteorological Office, 2018. Climatological data. Available.
953 http//en.vedur.is/climatology/data/, Accessed date: 13 April 2018.

954 Ingólfsson, Ó., Norddahl, H., 1994. A review of the environmental history of
955 Iceland, 13,000–9000 yr BP. J. Quat. Sci. 9, 147–150.
956 https://doi.org/10.1002/jqs.3390090208.

957 Ipsen, H.A., Principato, S.M., Grube, R.E., Lee, J.F., 2018. Spatial analysis of
958 cirques from three regions of Iceland: implications for cirque formation and
959 palaeoclimate. Boreas 47, 565–576. https://doi.org/10.1111/bor.12295.

960 Janke, J.R., 2005. Photogrammetric analysis of front range rock glacier flow rates.
961 Geogr. Ann. Ser. A, Phys. Geogr. 87, 515–526. https://doi.org/10.1111/j.0435-
962 3676.2005.00275.x.

963 Janke, J.R., Regmi, N.R., Giardino, J.R., Vitek, J.D., 2013. Rock glaciers. Treatise
964 on Geomorphology. Elsevier, pp. 238–273 https://doi.org/10.1016/B978-0-12-
965 374739-6.00211-6.

966 Janke, J.R., Bellisario, A.C., Ferrando, F.A., 2015. Classification of debris-covered
967 glaciers and rock glaciers in the Andes of central Chile. Geomorphology 241, 98–
968 121. https://doi.org/10.1016/j.geomorph.2015.03.034.

969 Jönsson, O., 1976. Berghlaup. Ræktunarfélag Norðurlands, Akureyri.

970 Kääb, A., 2002. Monitoring high-mountain terrain deformation from repeated air-
971 and spaceborne optical data: examples using digital aerial imagery and ASTER data.
972 ISPRS J. Photogramm. Remote Sens. 57, 39–52. https://doi.org/10.1016/S0924-
973 2716(02)00114-4.

974 Kääb, A., 2005. Remote sensing of mountain glaciers and permafrost creep.
975 Physische Geographie. Geographisches Institut der Universität Zürich.

976 Kääb, A., 2008. Remote sensing of permafrost-related problems and hazards.
977 Permafr. Periglac. Process. 19, 107–136. https://doi.org/10.1002/ppp.619.

978 Kääb, A., Haeberli, W., Gudmundsson, G.H., 1997. Analysing the creep of mountain
979 permafrost using high precision aerial photogrammetry: 25 years of monitoring
980 Gruben rock glacier, Swiss Alps. Permafr. Periglac. Process. 8, 409–426.
981 https://doi.org/10.1002/(SICI)1099-1530(199710/12)8:4b409::AID-
982 PPP267N3.0.CO;2-C.

983 Kääb, A., Kaufmann, V., Ladstädter, R., Eiken, T., 2003. Rock glacier dynamics:
984 implications from high-resolution measurements of surface velocity fields. In:

Phllips, M., Springman, S.M., Arenson, L.U. (Eds.), Proceedings of the Eighth International Conference on Permafrost. Balkema Publishers, Zurich, Switzerland, pp. 501–506.

Kaufmann, V., Ladstädter, R., 2003. Quantitative analysis of rock glacier creep by means of digital photogrammetry using multi-temporal aerial photographs: two case studies in the Austrian Alps. Proceedings of the 8th International Conference on Permafrost.

Kaufmann, V., Ladstädter, R., 2010. Documentation and visualization of the morphodynamics of Hinteres Langtalkar rock glacier (Hohe Tauern range, Austrian Alps) based on aerial photographs (1954–2006) and geodetic measurements (1999–2007). Grazer Schriften Der Geographie Und Raumforschung. 45, pp. 103–116.

Kellerer-Pirklbauer, A., Kaufmann, V., 2012. About the relationship between rock glacier velocity and climate parameters in central Austria. Austrian J. Earth Sci. 105, 94–112.

Kellerer-Pirklbauer, A., Wangensteen, B., Farbrot, H., Etzelmüller, B., 2007. Relative surface age-dating of rock glacier systems near Hólar in Hjaltadalur, northern Iceland. J. Quat. Sci. 23, 137–151. https://doi.org/10.1002/jqs.1117.

Kellerer-Pirklbauer, A., Lieb, G.K., Avian, M., Gspurning, J., 2008. The response of partially debris-covered valley glaciers to climate change: the example of the pasterze glacier (Austria) in the period 1964 to 2006. Geogr. Ann. Ser. A, Phys. Geogr. 90, 269–285. https://doi.org/10.1111/j.1468-0459.2008.00345.x.

Kellerer-Pirklbauer, A., Lieb, G.K., Kaufmann, V., 2017. The Dösen Rock Glacier in Central Austria: a key site for multidisciplinary long-term rock glacier monitoring in the Eastern Alps. Austrian J. Earth Sci. 110. https://doi.org/10.17738/ajes.2017.0013.

Kenner, R., Phillips, M., Beutel, J., Hiller, M., Limpach, P., Pointner, E., Volken, M., 2017. Factors controlling velocity variations at short-term, seasonal and multiyear time scales, Ritigraben rock glacier, Western Swiss Alps. Permafr. Periglac. Process. 28, 675–684. https://doi.org/10.1002/ppp.1953.

Kirkbride, M.P., 2000. Ice-marginal geomorphology and Holocene expansion of debriscovered Tasman Glacier, New Zealand. In: Nakawo, M., Raymond, C.F., Fountain, A. (Eds.), Debris-covered Glaciers. IAHS, pp. 211–217 Publication 264.

Kirkbride, M.P., 2011. Debris-covered glaciers. In: Singh, V.P., Singh, P., Haritashya, U.K. (Eds.), Encyclopedia of Snow, Ice and Glaciers: Encyclopedia of Earth Series. Springer, Netherlands, pp. 180–182 https://doi.org/10.1007/978-90-481-2642-2_622.

Lilleøren, K.S., Etzelmüller, B., Gärtner-Roer, I., Kääb, A., Westermann, S., Gumundsson, Á., 2013. The distribution, thermal characteristics and dynamics of permafrost in Tröllaskagi, northern Iceland, as inferred from the distribution of rock glaciers and ice-cored moraines. Permafr. Periglac. Process. 24, 322–335. https://doi.org/10.1002/ppp.1792.

Martin, E.H., Whalley, W.B., 1987. A glacier ice-cored rock glacier, Tröllaskagi, Iceland. Jökull 37, 49–56.

Martin, H.E., Whalley, W.B., Caseldine, C., 1991. Glacier Fluctuations and Rock Glaciers in Tröllaskagi, Northern Iceland, with special reference to 1946–1986. In:

Maizels, J.K., Caseldine, C. (Eds.), Environmental Change in Iceland: Past and Present. Springer Netherlands, Dordrecht, pp. 255–265 https://doi.org/10.1007/978-94-011-3150-6_17.

Martin, H.E., Whalley, B., Orr, J., Caseldine, C., 1994. Dating and interpretation of rock glaciers using lichenometry, south Tröllaskagi, North Iceland. Münchener Geogr. Arb. 12, 205–224.

Mercier, D., Cossart, E., Decaulne, A., Feuillet, T., Jónsson, H.P., Sæmundsson, Þ., 2013. The Höfðahólar rock avalanche (sturzström): chronological constraint of paraglacial landsliding on an Icelandic hillslope. The Holocene 23, 432–446. https://doi.org/10.1177/0959683612463104.

Monnier, S., Kinnard, C., 2015a. Geomorphology, internal structure, and successive development of a glacier foreland in the semiarid Chilean Andes (Cerro Tapado, upper Elqui Valley, 30°08′ S., 69°55′ W.)—reply to discussion by D.C. Nobes. Geomorphology 250, 461–463. https://doi.org/10.1016/J.GEOMORPH.2015.02.010.

Monnier, S., Kinnard, C., 2015b. Reconsidering the glacier to rock glacier transformation problem: new insights from the central Andes of Chile. Geomorphology 238, 47–55. https://doi.org/10.1016/J.GEOMORPH.2015.02.025.

Monnier, S., Kinnard, C., 2017. Pluri-decadal (1955–2014) evolution of glacier-rock glacier transitional landforms in the central Andes of Chile (30–33° S). Earth Surf. Dyn. 5, 493–509. https://doi.org/10.5194/esurf-5-493-2017.

Monnier, S., Camerlynck, C., Rejiba, F., Kinnard, C., Feuillet, T., Dhemaied, A., 2011. Structure and genesis of the Thabor rock glacier (Northern French Alps) determined from morphological and ground-penetrating radar surveys. Geomorphology 134, 269–279. https://doi.org/10.1016/J.GEOMORPH.2011.07.004.

Monnier, S., Kinnard, C., Surazakov, A., Bossy, W., 2014. Geomorphology, internal structure, and successive development of a glacier foreland in the semiarid Chilean Andes (Cerro Tapado, upper Elqui Valley, 30°08′ S., 69°55′ W.). Geomorphology 207, 126–140. https://doi.org/10.1016/J.GEOMORPH.2013.10.031.

Pelto, M., Capps, D., Clague, J.J., Pelto, B., 2013. Rising ELA and expanding proglacial lakes indicate impending rapid retreat of Brady Glacier, Alaska. Hydrol. Process. 27, 3075–3082. https://doi.org/10.1002/hyp.9913.

Pétursson, H.G., Norðdahl, H., Ingólfsson, Ó., 2015. Late Weichselian history of relative sea level changes in Iceland during a collapse and subsequent retreat of marine based ice sheet. Cuad. Investig. Geográfica 41, 261–277. https://doi.org/10.18172/cig.2741.

Potter, N.J., Steig, E.J., Clark, D.H., Speece, M.A., Clark, G.M., Updike, A.B., 1998. Galena Creek rock glacier revisited—new observations on an old controversy. Geogr. Ann. Ser. A, Phys. Geogr. 80, 251–265. https://doi.org/10.1111/j.0435-3676.1998.00041.x.

Roer, I., Nyenhuis, M., 2007. Rockglacier activity studies on a regional scale: comparison of geomorphological mapping and photogrammetric monitoring. Earth Surf. Process. Landf. 32, 1747–1758. https://doi.org/10.1002/esp.1496.

Roer, I., Kääb, A., Dikau, R., 2005. Rockglacier kinematics derived from small-scale aerial photography and digital airborne pushbroom imagery. Z. Geomorph. N.F 49, 73–87.

Sæmundsson, K., Kristjansson, L., McDougall, I., Watkins, N.D., 1980. K-Ar dating, geologicaland paleomagnetic study of a 5-km lava succession in northern Iceland. J. Geophys. Res. Solid Earth 85, 3628–3646. https://doi.org/10.1029/JB085iB07p03628.

Sæmundsson, Þ., Pétursson, H., Kneisel, C., Beylich, A., 2007. Monitoring of the Tjarnardalir landslide, in central North Iceland. In: Schaefer, V.R., Schuster, R.L., Turner, A.K. (Eds.), First North American Landslide Conference. AEG, Vail Colorado, pp. 1029–1040 Publication No. 23.

Seppi, R., Zanoner, T., Carton, A., Bondesan, A., Francese, R., Carturan, L., Zumiani, M., Giorgi, M., Ninfo, A., 2015. Current transition from glacial to periglacial processes in the Dolomites (South-Eastern Alps). Geomorphology 228, 71–86. https://doi.org/10.1016/j.geomorph.2014.08.025.

Shroder, J.F., Bishop, M.P., Copland, L., Sloan, V.F., 2000. Debris-covered glaciers and rock glaciers in the Nanga Parbat Himalaya, Pakistan. Geogr. Ann. Ser. A, Phys. Geogr. 82, 17–31. https://doi.org/10.1111/j.0435-3676.2000.00108.x.

Sigurdsson, O., 1990. Mödrufellshraun, berghlaup eda jökullrudningur? Náttúrufraedingurinn 60, 107–112.

Sigurðsson, O., Williams, R.S., 2008. Geographic names of Icelandic glaciers: historic and modern. US Geological Survey Professional Paper 1746.

Vitek, J.D., Giardino, J., 1987. Rock glaciers: a review of the knowledge base. In: Giardino, J.R., Shroder, J.F., Vitek, J.D. (Eds.), Rock Glaciers. Allen and Unwin, Boston, pp. 1–26.

Wahrhaftig, C., Cox, A., 1959. Rock glaciers in the Alaska Range. GSA Bull. 70, 383–436. https://doi.org/10.1130/0016-7606(1959)70[383:RGITAR]2.0.CO;2.

Wangensteen, B., Gudmundsson, Á., Eiken, T., Kääb, A., Farbrot, H., Etzelmüller, B., 2006. Surface displacements and surface age estimates for creeping slope landforms in Northern and Eastern Iceland using digital photogrammetry. Geomorphology 80, 59–79. https://doi.org/10.1016/j.geomorph.2006.01.034.

Whalley, W.B., Martin, H.E., 1992. Rock glaciers: II models and mechanisms. Prog. Phys. Geogr. 16, 127–186. https://doi.org/10.1177/030913339201600201.

Whalley, B., Martin, H.E., 1994. Rock glaciers in Tröllaskagi: their origin and climatic significance. In: Stötter, J., Willhelm, F. (Eds.), Environmental Change in Iceland. Münchener Geographische Abhandlungen, Germany, pp. 289–308.

Whalley, W.B., Douglas, G.R., Jonsson, A., 1983. The magnitude and frequency of large rockslides in Iceland in the postglacial. Geogr. Ann. Ser. A, Phys. Geogr. 65, 99–110. https://doi.org/10.2307/520724.

Whalley, W.B., Hamilton, S., Palmer, C., Gordon, J., Martin, H.E., 1995a. The dynamics of rock glaciers: data from Trollaskagi, North Iceland. In: Slaymaker, O. (Ed.), Steepland Geomorphology. John Wiley & Sons, pp. 129–145.

Whalley, W.B., Palmer, C.F., Hamilton, S.J., Martin, H.E., 1995b. An assessment of rock glacier sliding using seventeen years of velocity data: Nautárdalur Rock Glacier, North Iceland. Arct. Alp. Res. 27, 345–351. https://doi.org/10.2307/1552027.

Wirz, V., Gruber, S., Purves, R.S., Beutel, J., Gärtner-Roer, I., Gubler, S., Vieli, A., 2016. Shortterm velocity variations at three rock glaciers and their relationship with meteorological conditions. Earth Surf. Dyn. 4, 103–123. https://doi.org/10.5194/esurf-4-103-2016.

TABLES

Table 1. Absolute orientation obtained for each stereo-pair.

Flight date	Stereopairs	Image scale (aprox.)	Absolute orientation (RMSE)	
1946	AMS1002121014		0.991	
	AMS1002121015			0.391
	AMS1002121016			
27/08/1980	F45-F-9871		0.153	
	F45-F-9872			
06/08/1985	J10-J-1724	1:29,000	0.215	
	J10-J-1725			0.215
	J10-J-1726			
07/08/1994	N06-N-1078	1:29,000	0.166	
	N06-N-1079			0.251
	N06-N-1080			

1127 Table 2. Horizontal displacements measured on surface blocks of the Hóladalsjökull
1128 debris-covered glacier at different periods.

Time Period	Total Blocks	Geomorphologic Unit	Nº blocks/units	Minimun Velocity (m/year)	Maximun Velocity (m/year)	Average Velocity (m/year)	Standard deviation (σ)
1980-1994	270	Debris-Covered Glacier (DCG-1)	172	0.0248	1.1594	0.3312	0.1609
		Glacier-derived depressions (DCG-2a, b and c)	76	0.0651	1.5953	0.3063	0.2205
		Stable ground (SG-7a)	22	0.0010	0.1220	0.0519	0.0291
1946-1980	19	Debris-Covered Glacier (DCG-1)	11	0.1015	0.5121	0.2996	0.1223
		Glacier-derived depressions (DCG-2a, b and c)	4	0.0896	0.2454	0.1782	0.0588
		Stable ground (SG-7a)	4	0.0132	0.1348	0.0981	0.0496
1980-1985	266	Debris-Covered Glacier (DCG-1)	172	0.0165	1.5581	0.3260	0.1941
		Glacier-derived depressions (DCG-2a, b and c)	70	0.0722	0.9112	0.3027	0.1700
		Stable ground (SG-7a)	24	0.0152	0.2791	0.1017	0.0622
1985-1994	308	Debris-Covered Glacier (DCG-1)	205	0.0369	1.3998	0.3549	0.1699
		Glacier-derived depressions (DCG-2a, b and c)	77	0.0354	1.6173	0.3214	0.2295
		Stable ground (SG-7a)	26	0.0174	0.1554	0.0696	0.0352
1994-2000	51	Debris-Covered Glacier (DCG-1)	27	0.0613	0.5070	0.2505	0.1267
		Glacier-derived depressions (DCG-2a, b and c)	18	0.0517	0.4089	0.2412	0.1134
		Stable ground (SG-7a)	6	0.1167	0.3014	0.2144	0.0692

1129

1130

1131 Table 3. Elevation changes measured on surface blocks of the Hóladalsjökull debris-
1132 covered glacier for the period 1980-1994.
1133

Time Period	Total Blocks	Geomorphologic Unit	Nº blocks/ units	Elevation Changes Minimum	Elevation Changes Maximun	Elevation Changes Mean	Standard deviation (σ)
1980-1994	270	Debris-Covered Glacier (DCG-1)	172	-2.78	0.59	-0.72	0.6185
		Glacier-derived depressions (DCG-2a, b and c)	76	-3.11	0.35	-1.14	0.7154
		Stable ground (SG-7a)	22	-0.94	0.81	-0.20	0.4164

1134
1135

1136

Table 4. Horizontal displacement and elevation changes measured on surface blocks of the Fremri-Grjótárdalur and Hóladalsjökull rock glaciers for the period 1980-1994.

Time period	Total Blocks	Geomorphologic Unit	Nº blocks/ units	Minimun Velocity (m/year)	Maximun Velocity (m/year)	Average Velocity (m/year)	Standard deviation (σ)	Elevation Changes Minimum	Elevation Changes Maximun	Elevation Changes Mean	Standard deviation (σ)
1980-1994	308	Rock Glacier (RG-3)	21	0.003	0.1043	0.034	0.024	-0.63	0.35	-0.236	0.2521
		Upper West Lobes (RGW-4a)	49	0.0206	0.2905	0.1412	0.051	-1.91	0.34	-0.56	0.4678
		Upper Central Lobes (RGW-4b)	88	0.0031	0.2352	0.1155	0.053	-1.49	0.22	-0.4955	0.4114
		Lower Central-West Lobes (RGW-4c)	37	0.0043	0.075	0.031	0.020	-0.97	0.4	-0.3881	0.3351
		Upper East Lobe (RGE-5a)	23	0.0022	0.1336	0.0438	0.028	-1.16	0.55	-0.1804	0.4374
		Lower East Lobe (RGE-5b)	25	0.0015	0.050	0.0244	0.013	-0.31	0.51	0.1288	0.2077
		Talus-derived rock glaciers (RGT-6a and b)	9	0.0079	0.0517	0.0289	0.012	-0.54	0.51	-0.0488	0.3402
		All Fremri-Grjótárdalur units	231	0.0016	0.2905	0.0870	0.063	-1.91	0.55	-0.3756	0.4531
		Stable ground (SG-7b)	56	0.0050	0.0869	0.0301	0.017	-0.94	0.38	-0.2373	0.3114

1142

Table 5. Displacement of ridges (A) and furrows (B) of the Hóladalsjökull debris-covered glacier for the periods 1946-2000 and 1980-1994.

	1946-2000			**1980-1994**		
	Min distance (m)	**Max. distance (m)**	**Average distance (m)**	**Min distance (m)**	**Max. distance (m)**	**Average distance (m)**
Ridge						
1	16.2	16.57	16.38	5.23	5.28	5.25
2	11.66	16.18	14.73	1.6	3.88	3.01
3	17.47	9.63	13.13	3.36	5	4.32
4	12.81	14.33	13.78	3.08	3.43	3.22
5	10.36	16.28	13.26	0.96	2.73	1.94
6	12.09	16.82	14.96	1.06	3.87	2.51
7	10.87	20.3	14.96	1.57	3.79	2.55
8	12.67	15.0	13.83	0.77	1.81	1.43
9	-	-	-	4.29	5.14	4.77
10	15.85	22.33	20.27	1.8	5.58	2.92
11	9.42	13.51	11.25	1.87	4.05	2.96
12	-	-	-	1.78	2.52	2.15
13	-	-	-	2.43	4.76	3.03
14	-	-	-	2.6	4.02	3.27
15	-	-	-	1.88	3.31	2.63
16	-	-	-	3.09	5.93	4.59
17	-	-	-	1.75	4.45	3.23
Furrow						
1	4.12	10.52	7.41	5.23	5.28	5.26
2				1.6	4.43	3.01
3	10.67	12.19	11.60	3.36	5.19	4.33
4	10.66	12.42	11.33	3.08	3.43	3.22
5	14	21.08	17.46	0.96	2.73	1.94
6	14.97	24.16	18.61	3.87	1.06	2.51
7	14.87	17.14	16.26	1.57	3.79	2.55
8	12.59	15.28	14.10	0.77	1.81	1.44
9				4.29	5.14	4.78
10				1.8	5.58	2.92
11				1.87	4.05	2.96
12				1.78	2.52	2.15
13				2.43	4.76	3.04
14				2.6	4.02	3.27
15				1.88	3.31	2.63
16	6.17	8.48	7.60	3.09	5.93	4.59
17				1.75	4.8	3.23

1149 Table 6. Displacements of ridges (A) and furrows (B) of Fremri-Grjótárdalur rock
1150 glaciers for the period 1980-1994.

	1980-1994		
	Min distance (m)	**Max. Distance (m)**	**Average distance (m)**
Ridge			
1	0.99	2.80	1.75
2	0.93	3.15	2.06
3	0.64	4.61	1.75
4	0.90	2.46	1.78
5	0,45	1.71	1.12
6	0.58	1.85	1.03
7	0.72	2.74	1.55
8	0.39	1.47	0.86
9	0.72	1.51	1.12
10	0.36	2.35	0,98
Furrow			
1	0.64	1.62	1.15
2	1.42	3.25	2.02
3	1.92	3.47	2.57
4	0.67	1.61	1.07
5	0.91	3.13	2.10
6	1.07	4.56	2.40
7	0.57	2.43	1.50
8	1.74	2.83	2,28
9	1.54	2.35	1.86
10	0.94	2.72	1.86
11	1.43	2.34	1.82
12	1.88	2.19	2,03
13	0.68	1.39	1.07
14	1.48	3.01	1.93
15	0.93	1.36	1.22

1151

1152

1153 Table 7. Surface elevation differences of the geomorphological units identified.

1154

Glacier/ Geomorphologic Unit	**Positive changes**			**No changes (+0.25/-0.25 m)**	**Negative changes**		
	Area (m^2)	Average height variation (m)	Volume (m^3)	Area (m^2)	Area (m^2)	Average height variation (m)	Volume (m^3)
Hóladalsjökull glacier	**3,285,120.00**	**2.42**	**7,949,827.16**	**874,560.00**	**863,060.00**	**-0.82**	**-705,865.75**
Hóladalsjökull Ice and Snow area	1,495,641.00	3.44	5,147,824.76	62,167.00	118,823.00	-0.95	-113,260.32
Hóladalsjökull spoon-shape depression (DCG-2a,b and C)	368,390.00	1.36	500,665.67	173,866.00	295,672.00	-0.97	**-286,702.86**
Hóladalsjökull debris-covered glacier (DCG-1)	1,193,368.00	1.28	1,530,284.33	591,342.00	428,875.00	**-0.69**	**-294,510.19**
Hóladalsjökull Rock glacier (RG-3)	227,721.00	3.39	771,052.40	47,185.00	19,692.00	-0.58	-11,393.48
Fremri-Grjótárdalur glacier	**703,899.00**	**2.33**	**1,643,019.21**	**399,897.00**	**282,774.00**	**-0.69**	**-194,912.32**
Fremri-Grjótárdalur active static rock glaciers (RGW-4a, b and RGE-5a)	249,571.00	1.59	397,787.87	173,511.00	147,521.00	**-0.69**	**-101,353.87**
Fremri-Grjótárdalur glacier depression (RGW-4b y RGE-5a)	60,661.00	2.29	139,116.10	14,910.00	26,230.00	-0.72	-18,837.57
Fremri-Grjótárdalur fossil rock glacier (RGW-4c y RGE-5b)	78,570.00	1.29	108,580.83	122,479.00	96,860.00	-0.64	**-61,798.33**
Fremri-Grjótárdalur ice and snow area	267,307.00	3.45	923,447.04	53,658.00	2,900.00	-1.28	-3,724.84
Fremri-Grjótárdalur talus-derived rock glaciers (RGT-6a and b)	47,790.00	1.55	74,087.37	35,339.00	9,263.00	-0.99	-9,197.71

1155

1156

1157

1158

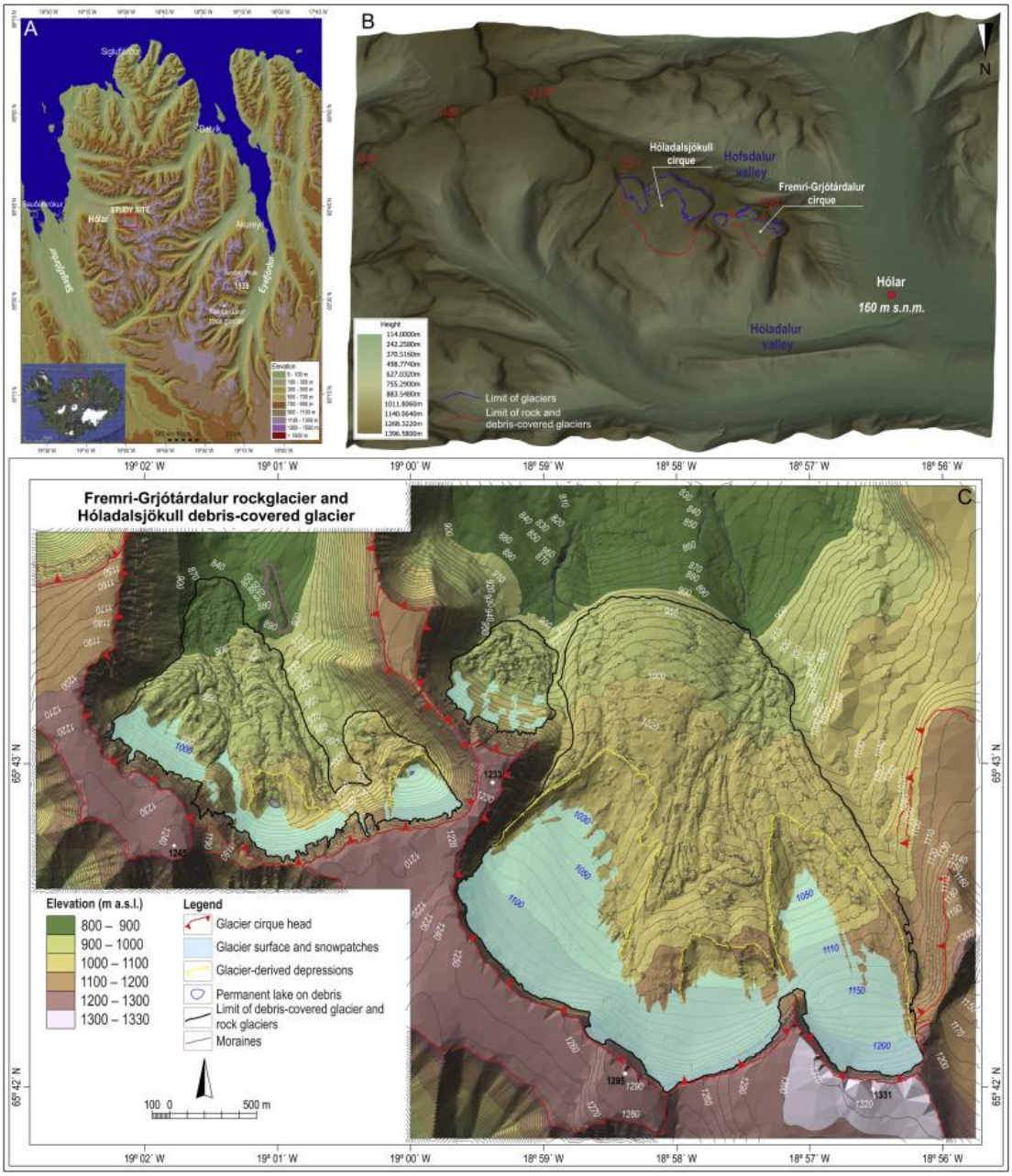
A
STUDY SITE
Hólar
B
N
Hóladalsjökull cirque
Hofsdalur valley
Fremri-Grjótárdalur cirque
Hólar
160 m s.n.m.
Hóladalur valley
Limit of glaciers
Limit of rock and debris-covered glaciers
C
Fremri-Grjótárdalur rockglacier and Hóladalsjökull debris-covered glacier
Elevation (m a.s.l.)
800 – 900
900 – 1000
1000 – 1100
1100 – 1200
1200 – 1300
1300 – 1330
Legend
Glacier cirque head
Glacier surface and snowpatches
Glacier-derived depressions
Permanent lake on debris
Limit of debris-covered glacier and rock glaciers
Moraines
100 0 500 m
19° 02´ W
19° 01´ W
19° 00´ W
18° 59´ W
18° 58´ W
18° 57´ W
18° 56´ W
65° 43´ N
65° 42´ N

1159

1160

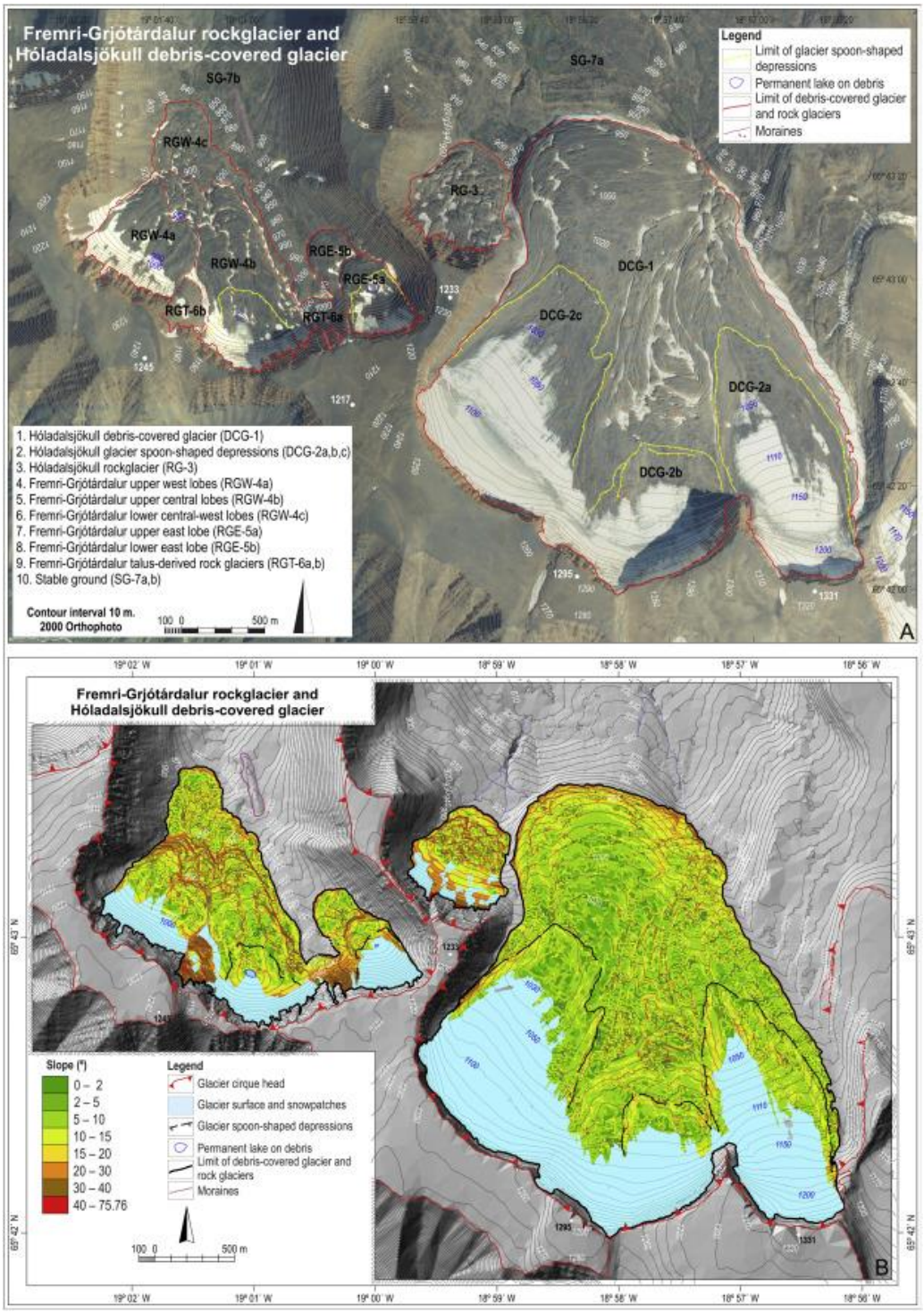
Fremri-Grjótárdalur rockglacier and Hóladalsjökull debris-covered glacier
SG-7b
SG-7a
RGW-4c
RG-3
RGW-4a
RGW-4b
RGE-5b
RGE-5a
RGT-6b
RGT-6a
DCG-1
DCG-2c
DCG-2a
DCG-2b
1233
1245
1217
1295
1331
Legend
Limit of glacier spoon-shaped depressions
Permanent lake on debris
Limit of debris-covered glacier and rock glaciers
Moraines
1. Hóladalsjökull debris-covered glacier (DCG-1)
2. Hóladalsjökull glacier spoon-shaped depressions (DCG-2a,b,c)
3. Hóladalsjökull rockglacier (RG-3)
4. Fremri-Grjótárdalur upper west lobes (RGW-4a)
5. Fremri-Grjótárdalur upper central lobes (RGW-4b)
6. Fremri-Grjótárdalur lower central-west lobes (RGW-4c)
7. Fremri-Grjótárdalur upper east lobe (RGE-5a)
8. Fremri-Grjótárdalur lower east lobe (RGE-5b)
9. Fremri-Grjótárdalur talus-derived rock glaciers (RGT-6a,b)
10. Stable ground (SG-7a,b)
Contour interval 10 m.
2000 Orthophoto
100 0 500 m
A
Fremri-Grjótárdalur rockglacier and Hóladalsjökull debris-covered glacier
Slope (°)
0 – 2
2 – 5
5 – 10
10 – 15
15 – 20
20 – 30
30 – 40
40 – 75.76
Legend
Glacier cirque head
Glacier surface and snowpatches
Glacier spoon-shaped depressions
Permanent lake on debris
Limit of debris-covered glacier and rock glaciers
Moraines
100 0 500 m
B

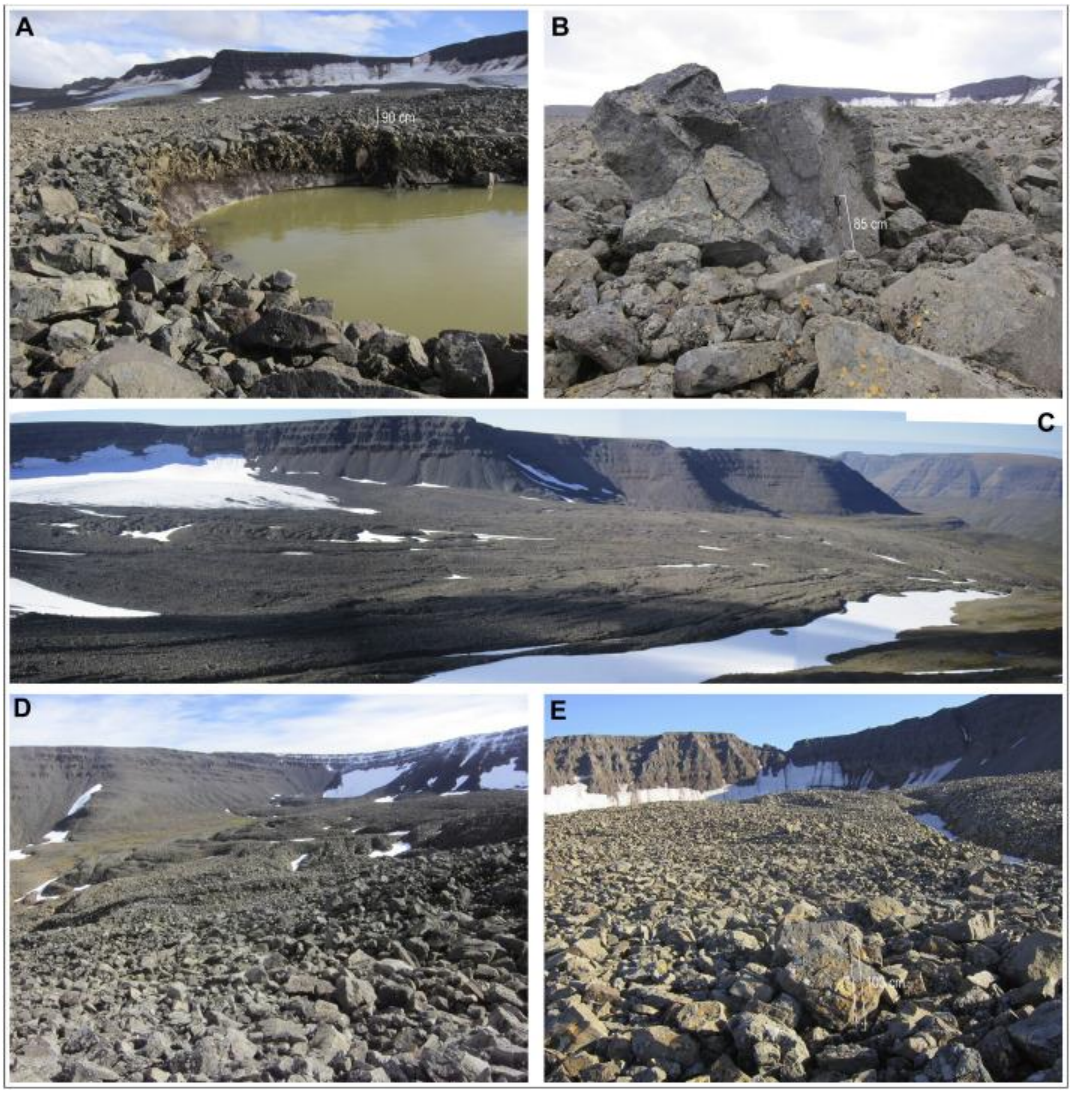

1163

1164

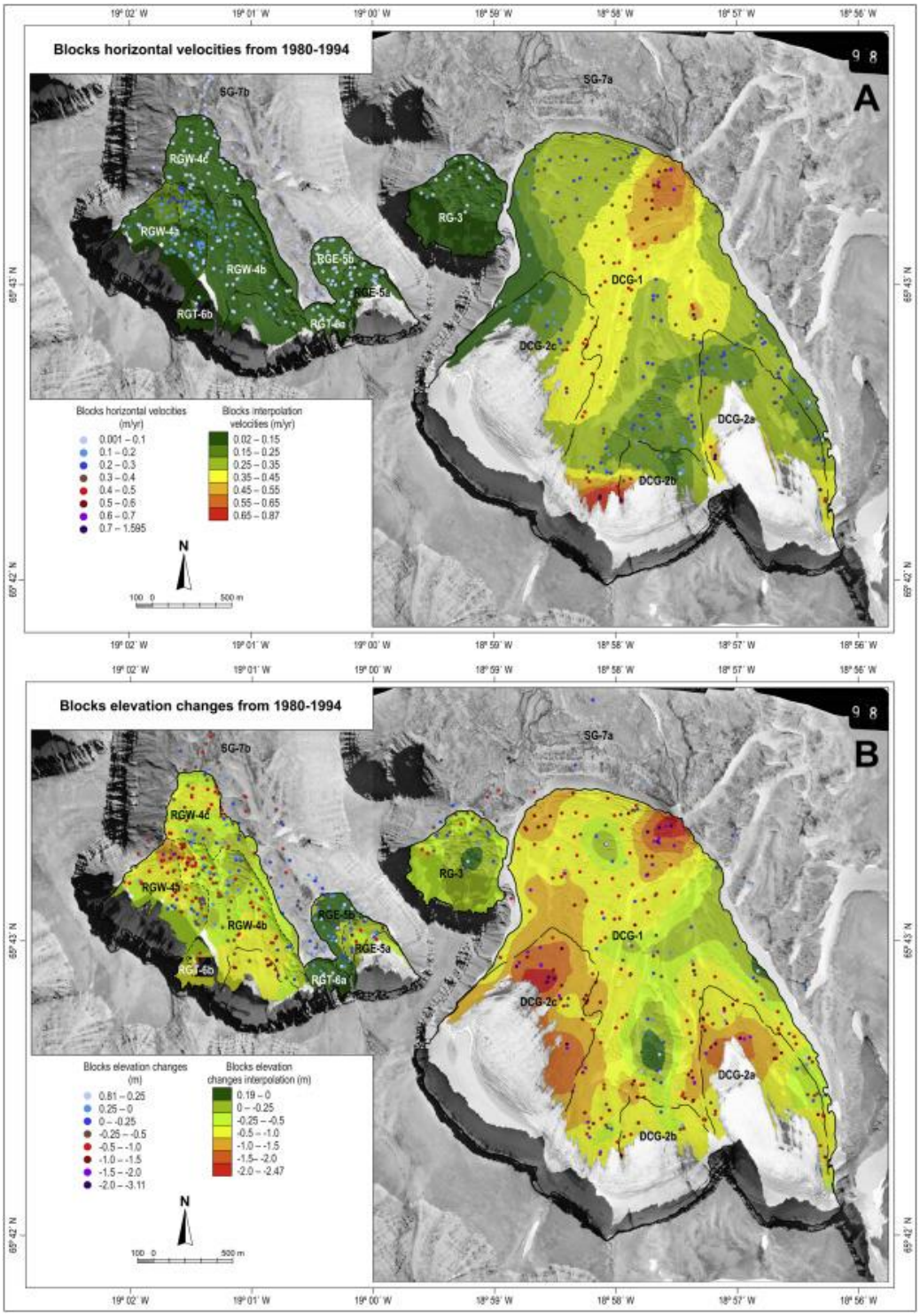
Blocks horizontal velocities from 1980-1994
A
SG-7a
SG-7b
RGW-4c
RGW-4a
RGW-4b
RG-3
RGE-5b
RGE-5a
RGT-6b
RGT-6a
DCG-1
DCG-2c
DCG-2a
DCG-2b
Blocks horizontal velocities (m/yr)
0.001 – 0.1
0.1 – 0.2
0.2 – 0.3
0.3 – 0.4
0.4 – 0.5
0.5 – 0.6
0.6 – 0.7
0.7 – 1.595
Blocks interpolation velocities (m/yr)
0.02 – 0.15
0.15 – 0.25
0.25 – 0.35
0.35 – 0.45
0.45 – 0.55
0.55 – 0.65
0.65 – 0.87
N
100 0 500 m
Blocks elevation changes from 1980-1994
B
Blocks elevation changes (m)
0.81 – 0.25
0.25 – 0
0 – -0.25
-0.25 – -0.5
-0.5 – -1.0
-1.0 – -1.5
-1.5 – -2.0
-2.0 – -3.11
Blocks elevation changes interpolation (m)
0.19 – 0
0 – -0.25
-0.25 – -0.5
-0.5 – -1.0
-1.0 – -1.5
-1.5– -2.0
-2.0 – -2.47
19° 02' W
19° 01' W
19° 00' W
18° 59' W
18° 58' W
18° 57' W
18° 56' W
65° 43' N
65° 42' N

1165

1166

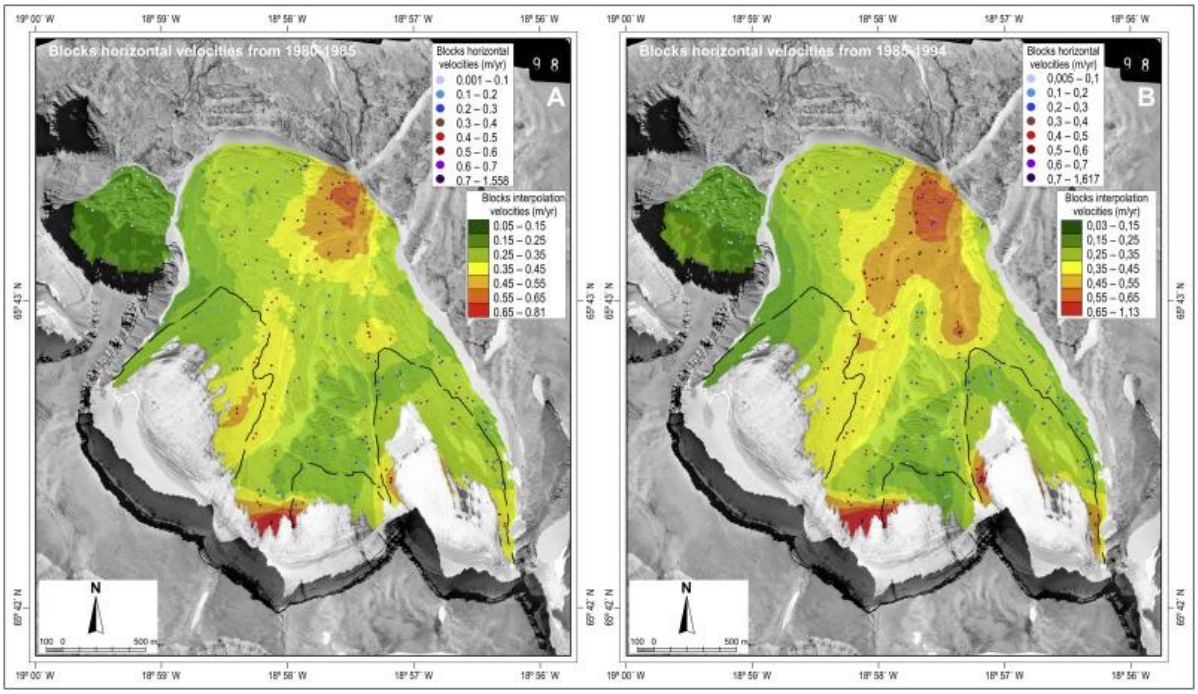
Blocks horizontal velocities from 1980-1985
Blocks horizontal velocities (m/yr)
0.001 – 0.1
0.1 – 0.2
0.2 – 0.3
0.3 – 0.4
0.4 – 0.5
0.5 – 0.6
0.6 – 0.7
0.7 – 1.558
A
Blocks interpolation velocities (m/yr)
0.05 – 0.15
0.15 – 0.25
0.25 – 0.35
0.35 – 0.45
0.45 – 0.55
0.55 – 0.65
0.65 – 0.81
N
Blocks horizontal velocities from 1985-1994
Blocks horizontal velocities (m/yr)
0,005 – 0,1
0,1 – 0,2
0,2 – 0,3
0,3 – 0,4
0,4 – 0,5
0,5 – 0,6
0,6 – 0,7
0,7 – 1,617
B
Blocks interpolation velocities (m/yr)
0,03 – 0,15
0,15 – 0,25
0,25 – 0,35
0,35 – 0,45
0,45 – 0,55
0,55 – 0,65
0,65 – 1,13
N

1167

1168

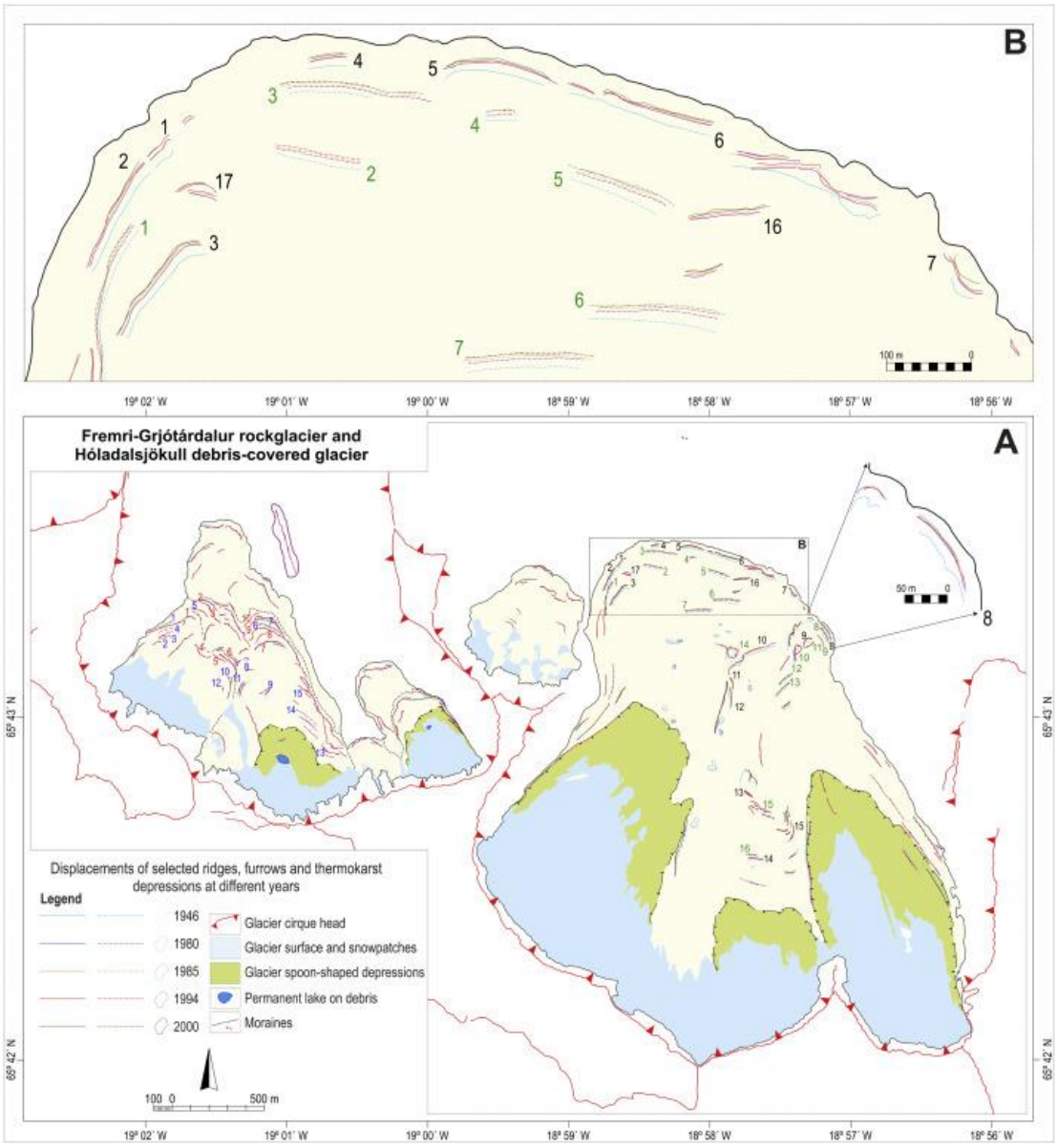
B
A
Fremri-Grjótárdalur rockglacier and
Hóladalsjökull debris-covered glacier
Displacements of selected ridges, furrows and thermokarst depressions at different years
Legend
1946
1980
1985
1994
2000
Glacier cirque head
Glacier surface and snowpatches
Glacier spoon-shaped depressions
Permanent lake on debris
Moraines
100 0 500 m
50 m 0
100 m 0
19° 02' W
19° 01' W
19° 00' W
18° 59' W
18° 58' W
18° 57' W
18° 56' W
65° 43' N
65° 42' N

1169

1170

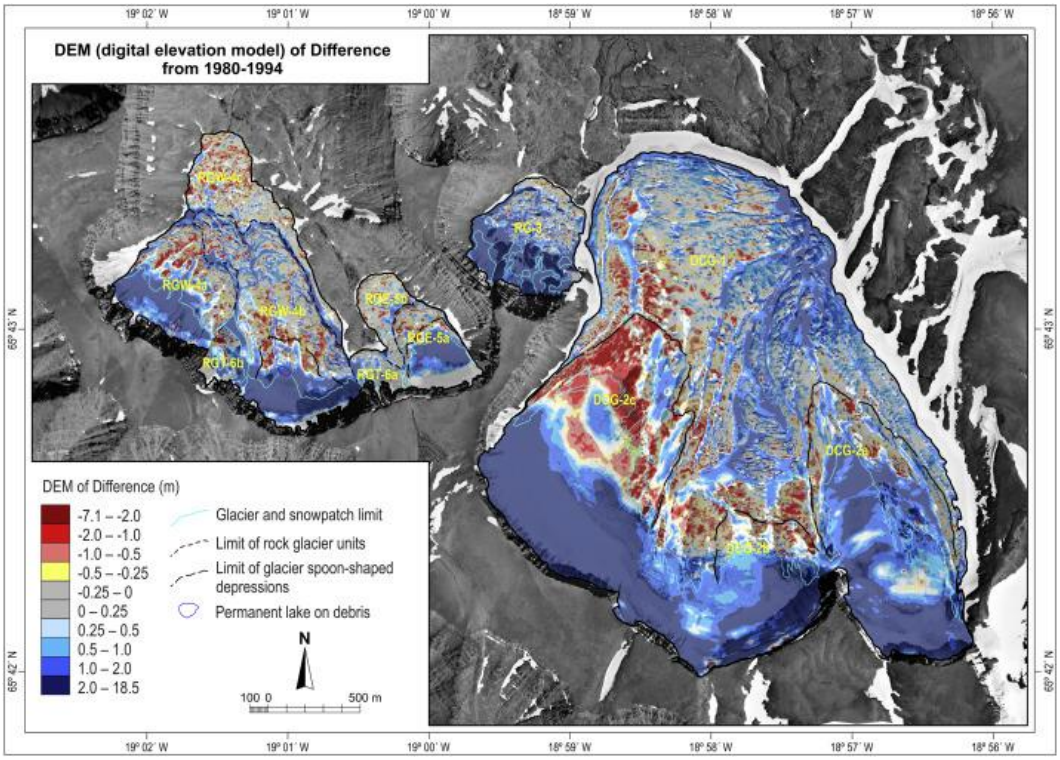
DEM (digital elevation model) of Difference from 1980-1994
19° 02' W
19° 01' W
19° 00' W
18° 59' W
18° 58' W
18° 57' W
18° 56' W
65° 43' N
65° 42' N
RGW-4a
RGW-3a
RGW-4b
RGW-5a
RGE-5b
RGE-5a
RG-3
DCG-1
DCG-2c
DCG-2b
DCG-2a
DEM of Difference (m)
-7.1 – -2.0
-2.0 – -1.0
-1.0 – -0.5
-0.5 – -0.25
-0.25 – 0
0 – 0.25
0.25 – 0.5
0.5 – 1.0
1.0 – 2.0
2.0 – 18.5
Glacier and snowpatch limit
Limit of rock glacier units
Limit of glacier spoon-shaped depressions
Permanent lake on debris
N
100 0
500 m

1171

1172

FIGURES

Figure 1. (A) Location of study area in theTrolläskagi Peninsula (northern Iceland); (B) 3D isometric view of Fremri-Grjótárdalur and Hóladalsjokull cirques at the head of the Holadalur valley, close to Hólar village; (C) High resolution digital elevation model of Fremri-Grjótárdalur and Hóladalsjokull cirques.

Figure 2. (A) Geomorphological units of the Fremri-Grjótárdalur and Hóladalsjokull cirques on the 2000 orthophoto; (B) Slope map of Fremri-Grjótárdalur rock glaciers and Hóladalsjökull debris-covered and rock glaciers.

Figure 3. Photographs showing some surface features. A) Recent formation of a thermokarst depression on the Hóladalsjökull debris-covered glacier. B) Large boulder on debris surface. C) Panoramic view of the debris-covered glacier surface, where long ridges and well-developed furrows can be seen. D) Detail of a Fremri-Grjótárdalur cirque rock glacier, where transversal ridges at the front can be observed. E) Gentle debris surface of a Fremri-Grjótárdalur cirque rock glacier. Photographs from August 2016.

Figure 4. Spatial distribution of horizontal block velocities (A) and elevation changes (B) 1980-1994 in the Hóladalsjökull debris-covered glacier and the Fremri-Grjótárdalur rock glacier.

Figure 5. Spatial distribution of horizontal block velocities in the Hóladalsjökull debris-covered glacier 1980-1985 (A) and 1985-1994 (B).

Figure 6. Map of selected ridges and furrows to measure displacement in Hóladalsjökull debris-covered glacier and Fremri-Grjótárdalur rock glacier from 1946 to 2000. General map of the cirques (A). Enlarged sector of the debris-covered glacier front (B).

Figure 7. Surface elevation differences derived from comparing 1980 and 1994 Digital Elevation Models, constructed from topographic maps scale 1:2000.